Professor Efstratios Pistikopoulos
Centre for Process Systems Engineering
Imperial College London

Professor Wolfgang Marquardt
Institute for Process Systems Engineering
RWTH Aachen University

Professor Constantinos Pantelides
Process Systems Enterprise
Managing Director

Integration of Model Based Optimal Design Methods in the Process Modeling Environment gPROMS

Diploma Thesis
by
Robert Pack

London, WS 2012/13

Task Description

Conceptual process design is a task of major importance within the development of new and the retrofit of existing processes. While there has been a lot of research on optimization-based process design such approaches are rarely integrated in industrial practise. Up to now simulation software is still the standard tool for conceptual design. In order to ease the implementation of optimization-based process design in industrial practise, the main goal of this thesis is to facilitate a superstructure-based process optimization within the process modelling environment gPROMS®, which is widely applied in industry. Therefore, firstly a superstructure formulation for a distillation column model needs to be implemented. In addition, as initialization plays a significant role during simulation and optimization, a robust, automated initialization procedure is an essential part of the model development. To finally determine an optimal process design an economic model of the process needs to be formulated and a solution strategy together with an adequate optimization algorithm need to be determined.

In order to validate the capabilities of the structural optimization approach the design of a cost-optimal cryogenic air separation process is chosen as an industrially relevant and complex case study. The process is highly coupled, in terms of energy and material streams, as it employs a double effect column along with a coupled side stripper column. This gives rise to challenges in terms of simulating and operating the process. Due to these complexities the process serves as an excellent example to illustrate the effectiveness of optimization strategies.

In addition to the structural optimization different aspects of process design or control can be coupled to or even directly be integrated within the optimization. Among those aspects are potentials for heat integration or the question of a suitable control structure. Furthermore several uncertainties arise from unknown process parameters such as changing feed conditions, product demands or the development of the market conditions. For all these aspects different methodologies have been proposed in the literature, which similar to the structural optimization are not really integrated in industrial practice yet. Most or at least some of the methodologies should therefore also be investigated within this thesis in order to identify their potential ease of integration and application in the process modelling environment gPROMS® to simultaneously optimize process and equipment to minimize the total process cost with user defined objective functions.

Prof. Efstratios Pistikopoulos

Prof. Dr.-Ing. Wolfgang Marquardt

Betreuer der Arbeit: Dipl. Ing. Mirko Skiborowski
Tag der Abgabe: 23.01.2013

Statutory Declaration

I herewith declare that I have completed the present thesis independently making use only of the specified literature and aids. Sentences or parts of sentences quoted literally are marked as quotations; identification of other references with regard to the statement and scope of the work is quoted. The thesis in this form or in any other form has not been submitted to an examination body and has not been published.

Date Signature

Eidesstattliche Erklärung

Hiermit versichere ich, dass die vorliegende Arbeit von mir selbständig angefertigt wurde und dass ich keine Hilfsmittel benutzt habe, die dem Aufgabensteller nicht bekannt sind. Ich erkläre mich damit einverstanden, dass die vorliegende Arbeit in der Lehrstuhlbibliothek und Datenbank aufbewahrt wird und für den internen Gebrauch kopiert werden darf.

Datum Unterschrift

Contents

List of Figures

List of Tables

Nomenclature

Constants

g	gravitational constant	$[\frac{m}{s^2}]$

Greek Letters

β	aeration factor	$[-]$
δ	film thickness	$[m]$
ϵ	packing void fraction	$[-]$
γ_i	liquid activity coefficient of component i	$[-]$
μ_G	vapour viscosity	$[Pa \cdot s]$
μ_L	liquid viscosity	$[Pa \cdot s]$
μ_S	isentropic expansion coefficient	$[\frac{K}{Pa}]$
μ_{JT}	*Joule-Thompson* coeffivcient	$[\frac{K}{Pa}]$
ν^D	reflux ratio	$[-]$
ν^R	boliup ratio	$[-]$
ν^{vap}	condenser vapour fraction	$[-]$
Φ	relative froth density	$[-]$
Ψ_{flood}	fractional allowed flooding	$[-]$
Θ	corrugation angle	$[rad]$
φ_i^0	reference vapour fugacity coefficient of component i	$[-]$
φ_i	vapour fugacity coefficient of component i	$[-]$
ζ_{ij}^F	splitting variable for feed i on stage j	$[-]$

ζ_j^R	splitting variable for reflux on stage j	$[-]$
ζ_{ij}^{SL}	splitting variable for liquid side draw i on stage j	$[-]$
ζ_{ij}^{SV}	splitting variable for vapour side draw i on stage j	$[-]$

Variables

Δp	pressure drop over entire column	$[Pa]$
δp_{dry}	dry pressure drop	$[\frac{Pa}{m}]$
Δp_{stage}	stage-wise pressure drop	$[Pa]$
$\dot{e}_{ij}$	energy flow of to equipment i from energy carrier j	$[kW]$
$\dot{m}_i$	mass flow of component i	$[\frac{kg}{s}]$
ℓ_{weir}	length of tray weir	$[m]$
a	annuity	[\$]
a_c	parameter in Peng-Robinson EOS	$[\frac{m^5}{mol^2 s^2}]$
A_j^{min}	minimum column area on stage j	$[m^2]$
A_{active}	active tray area	$[m^2]$
b	parameter in Peng-Robinson EOS	$[\frac{m^3}{mol}]$
C_B^i	reference cost of equipment i	[\$]
C_E^i	cost of equipment i	[\$]
C_{EC}^i	mass specific cost of energy carrier i	$[\frac{\$}{kW}]$
C_{RM}^i	mass specific cost of raw material i	$[\frac{\$}{kg}]$
C_0	initial value of an investment	[\$]
C_1	Reference equipment cost at time 1	[\$]
C_1	packing constant	[]
C_2	Reference equipment cost at time 2	[\$]
C_2	packing constant	[]

C_n	final value of an investment	[$]
C_P	total process cost	[$]
C_P^0	reference process cost	[$]
C_{0e}	Present value of all expenses	[$]
C_{0r}	Present value of all revenues	[$]
C_{column}	column cost	[$]
$C_{\text{internals}}$	cost of column internals	[$]
C_{platform}	platform cost	[$]
C_{EC}	total cost of energy	[$]
C_{FILL}	cost of raw materials to fill the process	[$]
C_{RM}	total cost of raw materials	[$]
C_{tower}	tower cost	[$]
D	degression coefficient	[−]
E	fractional weld efficiency	[−]
ent_j	fractional entrainment for 80% flooding on stage j	[−]
f_C^i	design complexity correction to equipment cost	[−]
f_M^i	material selection correction to equipment cost	[−]
f_P^i	pressure correction to equipment cost	[−]
f_T^i	temperature correction to equipment cost	[−]
f_i^L	liquid fugacity	[−]
f_i^V	vapour fugacity	[−]
F_j	feed molar flowrate to stage j	$[\frac{mol}{s}]$
F_j	feed to tray j	$[\frac{mol}{s}]$
F_{Pi}	compressibility factor of component i	[−]

FLV_j	Sherwood flow parameter on stage j	$[-]$
h_j^L	molar liquid enthalpy on stage j	$[\frac{J}{mol}]$
h_j^V	molar vapour enthalpy on stage j	$[\frac{J}{mol}]$
h_j^F	molar liquid feed enthalpy to stage j	$[\frac{J}{mol}]$
H^R	reflux enthalpy stream	$[\frac{J}{mol}]$
h_f	froth height	$[m]$
h_L	dimesionless holdup	$[-]$
h_w	weir height	$[m]$
h_{plate}	plate spacing	$[m]$
h_L^{reb}	reboiler liquid enthalpy	$[\frac{kJ}{kmol}]$
h_{ow}	height over weir	$[m]$
h_V^{reb}	reboiler vapour enthalpy	$[\frac{kJ}{kmol}]$
i	interest rate	$[\%]$
I_1	Cost index at time 1	$[-]$
I_2	Cost index at time 2	$[-]$
$K1$	empirical coefficient	$[-]$
K_{ij}	equilibrium constant of component i on stage j	$[-]$
L_j	liquid flow from tray j	$[\frac{mol}{s}]$
L_j	molar liquid flowrate form stage j	$[\frac{mol}{s}]$
l_{ij}	liquid molar flowrate of component i from stage j	$[\frac{mol}{s}]$
L_{reb}^{in}	liquid reboiler influx	$[\frac{kmol}{s}]$
L_{reb}^{out}	liquid reboiler outflow	$[\frac{kmol}{s}]$
m	parameter in Peng-Robinson EOS	$[-]$
M^i	equipment specific factor -	[

n_C	number of components	$[-]$
n_F	number of feeds	$[-]$
n_i^{reb}	molar holdup of component i in reboiler	$[kmol]$
n_j^L	liquid molar holdup on stage j	$[mol]$
n_j^V	vapour molar holdup on stage j	$[mol]$
n_S	number of column stages	$[-]$
n_E	number of process units	$[-]$
n_{ij}	holdup of component i on stage j	$[mol]$
n_{RM}	number of different raw materials	$[-]$
n_{SL}	number of liquid side-draws	$[-]$
n_{SV}	number of vapour side-draws	$[-]$
NPV	Net present value	[\$]
p	pressure	$[Pa]$
p	system pressure	$[Pa]$
p_i^S	vapour pressure of component i	$[Pa]$
p_D	design pressure	$[psig]$
p_O	operating pressure	$[psig]$
POT	payout time	$[a]$
q	interest factor	$[-]$
Q^i	specific quantity for equipment i	$[variable]$
Q_B^i	equipment specific reference quantity	$[variable]$
Q_P	process capacity	$[\frac{kg}{h}]$
Q_P^0	reference process capacity	$[\frac{kg}{h}]$
ROI	return on investment	$[-]$

S	corrugation side	$[m]$
S	maximum allowable stress	$[psi]$
S_j^L	molar liquid side-draw flowrate form stage j	$[\frac{mol}{s}]$
s_j^L	dimensionless liquid side-draw from stage j	$[-]$
S_j^V	molar vapour side-draw flowrate form stage j	$[\frac{mol}{s}]$
s_j^V	dimensionless vapour side-draw from stage j	$[-]$
S_j^L	liquid side flow from tray j	$[\frac{mol}{s}]$
S_j^V	vapour side flow from tray j	$[\frac{mol}{s}]$
T^{bub}	bubble point temperature	$[K]$
T^{dew}	dew point temperature	$[K]$
T^{sub}	sub-cooling temperature	$[K]$
t_p	shell thickness die to pressure	$[in]$
t_s	tower shell thickness	$[in]$
t_w	thickness wind and earthquake correction	$[in]$
t_{op}	time of process operations	$[s]$
U_j	internal energy holdup on stage j	$[J]$
U_{reb}	reboiler internal energy holdup	$[kJ]$
v_G	vapour velocity	$[\frac{m}{s}]$
V_j	molar vapour flowrate form stage j	$[\frac{mol}{s}]$
V_j	vapour flow from tray j	$[\frac{mol}{s}]$
v_j^{flood}	flooding velocity on stage j	$[\frac{m}{s}]$
v_L	liquid velocity	$[\frac{m}{s}]$
v_{ij}	vapour molar flowrate of component i from stage j	$[\frac{mol}{s}]$
V_{reb}^{out}	vapour reboiler outflow	$[\frac{kmol}{s}]$

V_{stage}	stage volume	$[m^3]$
W_{tower}	weight of a tower	$[lbs]$
x_{ij}	liquid mole fraction of component i on stage j	$[-]$
x_i^{reb}	reboiler liquid mole fractions	$[-]$
y_{ij}	vapour mole fraction of component i on stage j	$[-]$
y_i^{eq}	equilibrium vapour concentration of component i on stage j	$[\frac{mol}{mol}]$
y_i^{reb}	reboiler vapour mole fractions	$[-]$
z_{ij}^{L}	feed mole fraction to stage j	$[-]$

Abstract

here comes an abstract

1 Introduction

The scope of this thesis is to implement and examine model based optimal design methods in the process model environment gPROMS®. In order to achieve this, an example process is chosen to serve as a basis for demonstrating general capabilities for structural optimization approaches on complex processes.

Distillation columns are to this day the most prominent way for separating liquid mixtures. Vast amounts of energy are used during the separation of various product streams. In fact often the majority of the energy required in a given chemical process is consumed in the separation stage. Therefore separation sequences have been under investigation for many years. The synthesis of separation sequences poses great challenges, especially if complex multi-component mixtures are considered.

Several shortcut methods have been developed for screening of potential separation sequences. If several flowsheet alternatives are constructed it becomes necessary to further investigate, which is the most suited for requirements of the separation task at hand. To do so rigourous process models which incorporate tray-by-tray balances and non-ideal equilibria are employed. One approach, which is currently still carried out in industry practice, is to conduct a sequence of process simulations to find the most promising configuration in a manual, trial and error based procedure. However this approach is unlikely to yield near optimal results.

The more reliable alternative to synthesize near optimal flow sheets is to perform mathematical optimization on a process superstructure. In that context continuous decisions such as operating pressure or temperatures, as well as discrete decisions associated with structural choices on the process equipment have to be made. The resulting problems are called mixed-integer non-linear programs (MINLP), which pose considerable challenges in their solution process. Due to that structural optimization is carried out by experts, with careful consideration when setting up the problem and optimization in specialized programs.

On the other hand process simulation in flowsheeting environments such as Aspen Plus® or gPROMS® is an integral part of industrial practice. Hence the scope of this thesis is to implement a flexible, easily deployed model for process optimization in the aforementioned modeling environment gPROMS®, which is capable of automated model initialization as well as structural optimization. The implemented models will then be applied to the cryogenic air separation process. This process is used to produce highly pure nitrogen, oxygen and noble gases such as argon. While the components themselves do not display any severe non-idealities, the process is highly integrated and coupled in terms of energy and material streams. The column configuration features multiple feeds and side draws in conjunction with a side stripping section. This makes it especially challenging in terms of process optimization.

The following thesis is structured in six chapters. After these introductory remarks follows a closer look at the cryogenic air separation process, chosen as a demonstrative example for this thesis. The subsequent two chapters are dedicated to the mathematical representation of various units associated with the air separation process. While applied to the example, these models are implemented in a general form to be applicable to various different processes. Sec. 3 first introduces general concepts of evaluating chemical processes before discussing specific costing models for the case at hand. The models concerning operation of the process are presented in sec. 4. Aside from a steady-state and a dynamic model formulation, the actual model implementation is also dealt with in this chapter. To ascertain the capabilities of the implemented models, they are applied to several simulation and optimization cases, which are summarized in sec. 5. The final chapter summarizes significant parts of the thesis and provides suggestions for further investigation in the matter.

2 Example process

To investigate optimization techniques an example process to which they can be applied is needed. The cryogenic air separation process serves well as a demonstrative case. This process is highly complex due to a high degree of material and energy integration as well as extreme operating conditions.

This chapters first aims at providing some background on different air separation technologies, which are discussed in the first section. Afterwards a concrete process flowsheet, which will be referred to in the remainder of this thesis, is introduced and examined.

2.1 Air separation technology

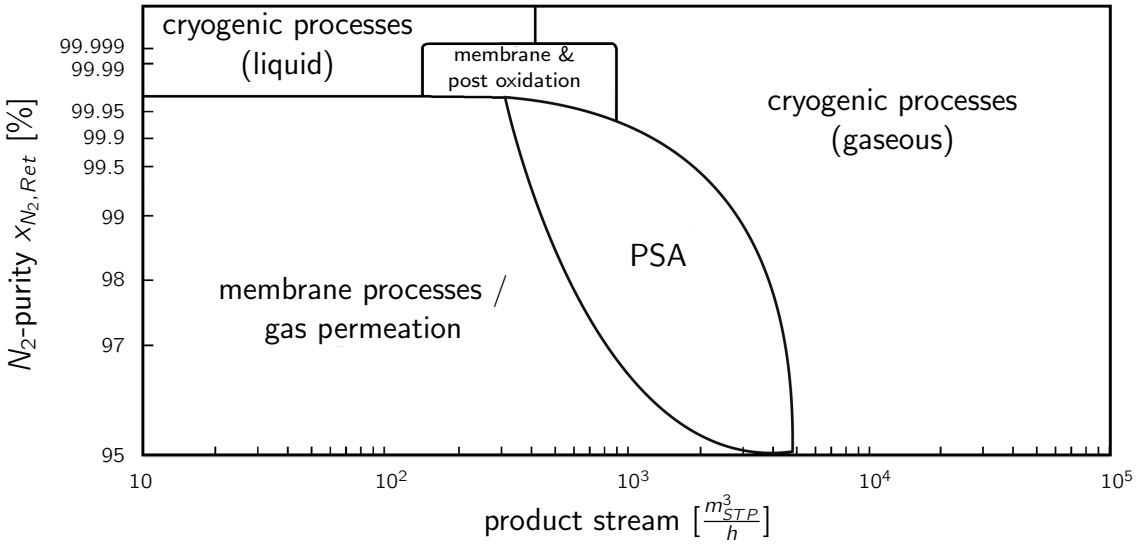

Figure 2.1: Comparison of Air Separation Technologies [37].

The separation of air finds many application in the modern industry. Pure oxygen and nitrogen are are essential for many processes. The yearly amount of oxygen extracted from air exceeds 100 million tonnes and nitrogen even surpassing these numbers [13]. Among the most prominent examples is the production of synthesis gas, which forms the basis for a multitude of very large-scale process operations. In addition the air separation processes find application as a utility provider rather than producer for example in highly efficient integrated combustion cycles [28]. Due to the many different applications, pure nitrogen or oxygen is needed with various demands on purity, flow rate or phase composition. Therefore different technologies are suitable to specific tasks.

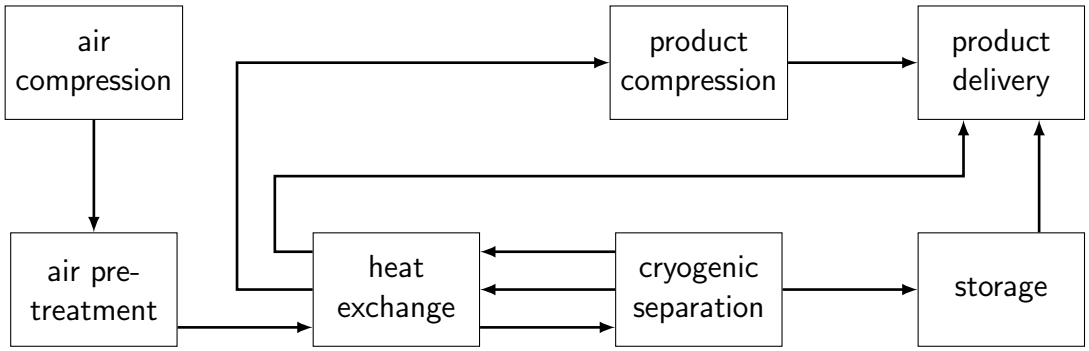

Figure 2.2: Schematic representation of the cryogenic air separation process.

In general three main principles of air separation can be identified; adsorption, cryogenic distillation and transport through membranes. Fig. 2.1 illustrates the economically most viable processes depending on product stream volume and purity. In the further course of this chapter the most prevalent air separation technologies along with their main fields of application and economic scope are introduced.

2.1.1 Cryogenic processes

Cryogenic air separation processes are implemented over a great variety of industries among others refining, petrochemicals, medical, food & beverages and environmental [41]. Fig. 2.2 shows the major unit operations associated with the process. Initially the air is compressed and later re-expanded to reach the low temperatures required for liquefaction. In an intermediate pre-treatment step most unwanted contaminants are removed. Particularly the amount of carbon dioxide in the gas carries great significance, as operating conditions lie beneath its freezing point. Due to freeze out at those low temperatures, especially within the heat exchanger the performance of process units can greatly be reduced, or entirely hindered. The pre-treated air is then cooled against product streams leaving the separation stage of the process. To which extend the refrigeration is recovered is among the most dominant factors for economic operations. The requirements towards the product streams determine how much can be recovered. Most processes produce gaseous streams at approximately ambient pressure and temperature [42] and hence recover the maximum of energy from the process. However often a subsequent compression step or even liquefaction step is employed to deliver the desired product to the consumer.

In terms of economically feasible operations, the compression denotes a sizable contribution to the capital cost and is responsible for the majority of the operating cost. However when recovering liquid product, the compression work needs to increase in order to compensate for the loss in recoverable refrigeration. Due to the widespread application of the process, several increasingly complex process configurations are being implemented with different strategies, for internal recovery of pressure energy and refrigeration.

The cryogenic process can most economically simultaneously produce large quantities of highly pure oxygen and nitrogen. In addition argon and other noble gases can be recovered from the process. Most alternative technologies will produce one single product stream. Additionally the economy of scale can very well be exploited for this process, which is why current developments are towards large

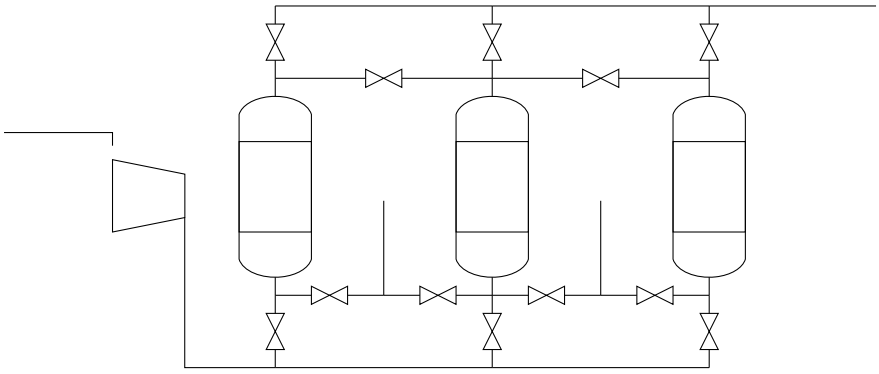

Figure 2.3: Schematic representation of a three bed PSA process.

scale single train that can produce an excess of several thousand tonnes of product stream per day [7].

2.1.2 Adsorption processes

Certain materials display a higher affinity to adsorb a specific class of molecules. Nitrogen is more easily adsorbed in zeolites than oxygen. Therefore if air is fed through a zeolite bed, an oxygen rich stream is produced. Since any bed will eventually be saturated and its capability for adsorption be exhausted, the process carries an inherent discontinuity. However, for most processes which yield large product streams, continuous operations are more cost effective.

To realize a continuous process multiple adsorption vessels are operated simultaneously. Once a bed is saturated, the process is switched to a different vessel and the saturated one is regenerated. Regeneration utilizes the change of adsorption capabilities at varying temperature or pressure. By increasing temperature or lowering pressure can the bed therefore be regenerated. Due to the switching during operations these processes a commonly known as Temperature Swing Adsorption (TSA) or Pressure Swing Adsorption (PSA). For most industrial applications PSA is preferred for its simpler operation and faster cycle times [42].

The ability to construct very compact units, have led to implementations of PSA processes at very different scales. Briefcase sized units are constructed for treatment of asthma patients or other medical appliances. Larger scale plants have successfully been utilized, for example in the paper industry during the de-lignation of pulp [34].

The bed size is the determining factor for equipment cost. Since cycle times are limited by the regeneration step, the bed size and therefore the cost increases rapidly with the product flowrate. For very large scale operations the cryogenic process is more economically viable. However the PSA/TSA process can be operated much more flexible due to drastically shorter start-up times compared to the cryogenic process. Furthermore, no by-products can be recovered from the process without further subsequent separations [9].

Fig. 2.3 shows a simple flowsheet of a PSA process. For continuous operations two separate beds would suffice, however, to expedite cycle times and process throughput as well as exploit possibilities for pressure energy recovery, process configurations with three or more beds are often installed.

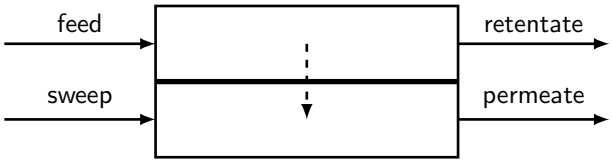

Figure 2.4: Membrane unit for gas permeation.

Variations of the process use sub-atmospheric pressures during the regeneration step. Such processes are commonly referred to as Vacuum Swing Adsorption (VSA).

2.1.3 Membrane processes

In case of the membrane process, the type of membrane used leads to very different process characteristics. For the production of oxygen either polymeric membranes (PEM) or ion-transport membranes (ITM) are installed.

Polymeric membranes operate at near ambient conditions. The driving force for separation is the difference in diffusion rates through the membrane [32]. The product flowrate and selectivity are the determining factors for capital cost. These are mainly dependent on the membrane area. Hence the capital cost for the process is expected to rise somewhat linear with the product flowrate. The process can economically generate a medium process stream ($\approx 20\ t/d$) at lower purities. The minimal start-up time and operations near ambient conditions make the process ideal for applications where oxygen enriched process streams suffice and contaminants such as water or carbon dioxide can be tolerated. Membranes which incorporate active species that facilitate oxygen transport trough the membrane bear the potential to greatly improve process performance [20]. In general though, the alternative technologies are more mature than membrane processes.

Processes with ion exchange membranes are drastically different from the ones with PEM's. Foremost they operate at high temperatures ($\approx 900K$). At the membrane surface oxygen molecules are ionized and transported through the membrane along an externally applied electric potential. They travel through the membrane at very high flow rates. The process is capable of producing virtually pure oxygen. It is especially suited for integration with power generation processes [42].

2.1.4 Hybrid processes

The three different alternatives presented before constitute the major technologies for separations of gases and therefore the production of pure nitrogen and oxygen. All technologies have their specific advantages and disadvantages. As the separation of gases remains a major issue when facing upcoming challenges for our industries substantial efforts are being made to improve current processes in terms of ecological and economic performance. A very promising way to achieve such improvements is to combine these technologies to form hybrid processes. Membranes offer many favourable characteristics are subject to limitations when it comes to large flow-rates and high purities. When lower purities are required or the flow-rates are limited they offer an efficient and cost effective way for gas separation. Therefore in the past years several alternatives for PSA - membrane [1] or

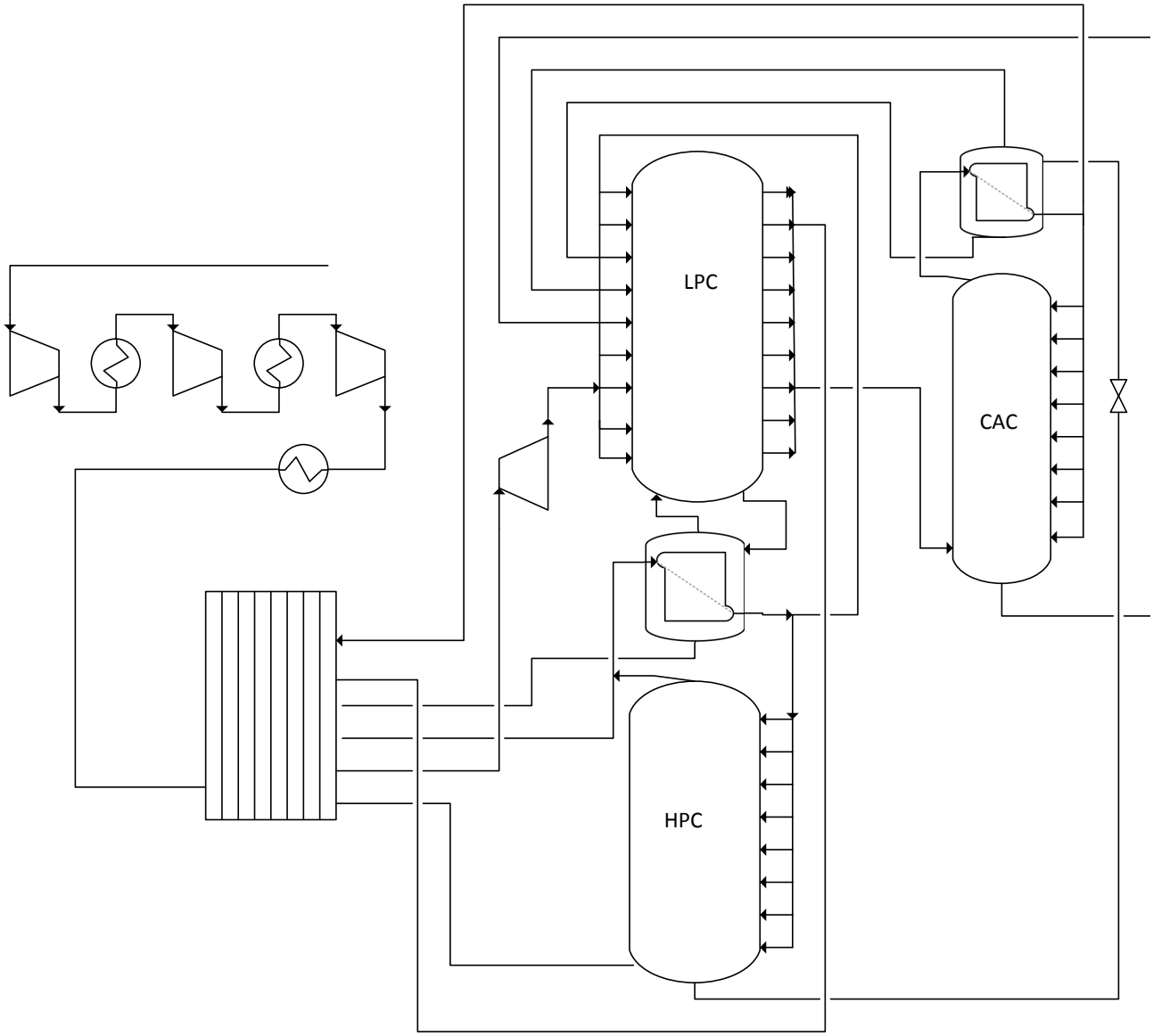

Figure 2.5: Example process superstructure.

membrane-cryogenic distillation processes [44] have been studied. The membrane can function within the process either as a pretreatment step, where a product enriched stream at medium purities and high flow-rates is produced, or after the main separation, when the main by-products are already removed, as a last stage to reach very high purities.

2.2 Air separation unit

The developed models were combined to a process flowsheet for the cryogenic air separation process. As no specific process was being evaluated, the process configuration was modeled after an published example process flowsheet [22]. Fig. 2.5 shows the flowsheet considered henceforth. Air is drawn from the surrounding at ambient conditions and compressed with inter-cooling stages. Afterwards the entering process stream exchange heat with the product streams.

The stream is then divided into two separate streams. One part is expanded in a turbine, and fed to the low pressure column (LPC) while the majority is fed to the high pressure column (HPC). Condenser and reboiler are combined in a single unit. A side column to the LPC generates pure argon. The condensate form the HPC is partially fed into the LPC. The oxygen rich sump product form the HPC is used to condensate the CAC top product, and afterwards fed into the LPC. From the reboiler side liquid oxygen is recovered from the process. From the top of LPC and HPC gaseous nitrogen is drawn. Liquid Argon is drawn from the CAC condenser.

AS can be seen, this process is highly integrated with respect to energy and material streams. For both the steady-state and dynamic process model, the same separation sequence is considered. Compression and heat-exchange are only explicitly modeled in the steady-state process. While the steady-state models do provide the possibility to calculate pressure drops by means of an hydraulic model, they were assumed constant in all steady-state applications. When using the dynamic models, hydraulic equations have to be considered. For the case of the ASU process different column internals are often installed. The HPC as the smallest column can be economically operated as a trayed column, hence the respective hydraulic and cost models were employed there. The LPC and CAC are mostly equipped with structured packings.

Another difference in the steady-state and dynamic models was the considered superstructure. For optimizing the number of separation stages, a maximum value needs to be guessed. In the steady-state case those were set to 40 for the HPC and 60 for the LPC and CAC respectively. With the steady-state results in mind, these were reduced to 25 for the HPC and 45 for LPC and CAC when constructing the dynamic process.

3 Process economics

Aside from question whether a certain process is capable of producing products according to specifications, it needs to be investigated if it does so while meeting economic criteria. The modeling of process economics is a powerful tool to estimate project profitability. Knowledge of process economics is mostly regarded for three types of decisions

- Compare design options with regard to profitability.
- Economically optimize a given design.
- Estimate project profitability

In any case the total cost of a given project as well as the cash flow structure will have to be analyzed to supply the decision maker with an accurate estimate of the economic conditions. To do so, adequate measures to compare and analyze a project in economic terms need to be implemented.

It is evident that, as the more information about a given process becomes available, any cost can be estimated more accurately. During the design phase of a process roughly three different qualities of cost estimation can be identified.

- An estimate before designing the process yields an order of magnitude estimation for supporting market research efforts. (Error $> 30\%$)
- An estimate in the early design phase based on essential process equipment. (Error $\pm 30\%$)
- An estimate based on an advanced flowsheet and relevant process parameters. (Error $\pm 20\%$)

Once detail engineering commences, even more accurate calculations with errors reducing to $\pm 5\%$ can be undertaken[36]. At that point a concrete process option will have to be chosen and the investment decision, hence the go-ahead for the project, will already have to be made. All optimization measures within the scope of this thesis will already have concluded at that time.

Within sec. 3.1 first we will take a look at how the total cost of a chemical process might be estimated at different design stages. Subsequently in sec. 3.2 some different ways of evaluating and comparing investment options will be discussed. The last section is then concerned with concrete costing and sizing models used for simulation and optimization purposes.

3.1 Evaluation of chemical processes

An important factor in every given project is the total cost. During the design of a chemical process many important aspects of the future cost structure are not known a priori, as the final design is still

under development. In general the total cost of implementing and operating a production site can be broken down into several subcategories.

- Battery limit investment
- Utility investment
- Off-Site investment
- Engineering fees
- Working capital

The subsequent sections will present an overview as to how these different costs can be approximated depending on the level of detail of the information provided.

3.1.1 Before process design

Before any details about the process to be implemented are known, an estimate can only give an order of magnitude towards cost to be expected. The cost of the new process C_P can be related to the cost of a reference process C_P^0 by

$$C_P = C_P^0 \cdot \left(\frac{Q_P}{Q_P^0} \right)^D , \tag{3.1}$$

where the quantity Q refers to a specific process quality. In most cases a production rate or total annual capacity will be used. The degression coefficient D needs to be correlated from historical data.

As the overall price structure will change over time, the reference price will not reflect the current market situation. In order to adjust for that shortcoming several price indices are published all over the word. Some of those tailor to special branches of the industry, others give a picture of the price-development in an economy as a whole. The ratio of prices levels at different times is then assumed to be equal to the ratio of the price indices at the respective times

$$\frac{C_1}{C_2} = \frac{I_1}{I_2}. \tag{3.2}$$

For each index an somewhat arbitrary reference year is chosen. Among the most common indices are the Marshall & Swift index, the Nellson-Farrar-Index or the Chemical Engineering index. Some exemplary values for these indices are given in tab. 3.1. As one can see the development within the process industry very well matches the development in the economy as a whole, which is why for this rough estimate general indices should suffice.

3.1.2 During process design

Once the future design has been broken down to fewer potential options and first process flowsheets are available, a more elaborate approach, resulting in much improved estimates, becomes possible. In contrast to the most general case, now the aforementioned investment areas can be distinguished. The following sections describe how estimates are attained for the respective investment category.

	Marshall & Swift Equipment Index 1926 ≡ 100		Nelson-Farrar Refinery Construction Index 1946 ≡ 100	Chemical Engineering Plant Cost Index 1957 ≡ 100
year	all industries	process industry		
1975	444	452	576	182
1980	560	675	823	261
1985	790	813	1074	325
1990	915	935	1226	358
1995	1027	1037	1392	381
2000	1089	1103	1542	394
2001	1093	1107	1565	396

Table 3.1: Price indices and their development.[10]

Battery limit investment

The battery limit investment denotes all investments necessary to have all required equipment for process operations installed on-site. This includes structures necessary to house the process as well as delivery and installation of all individual assets. One major part of these cost will the the process equipment. As the exact manufacturers and models of the equipment will not be known in early design stages, an approximation similar to the one in sec. 3.1.1 still needs to be employed. In contrast to before now the cost for individual pieces of process equipment will be considered explicitly. Each piece of equipment will have an specific feature which most heavily affects its cost. For vessels and reactors this might be volume, while for heat exchangers the required heat exchange area determines size and price of the unit. Accordingly, the price for an piece of equipment i C_E^i can again be approximated by a simple power law

$$C_E^i = C_B^i \left(\frac{Q_E^i}{Q_B^i} \right)^{M^i} . \tag{3.3}$$

A reference price C_B^i is multiplied by the determining quantity Q^i normalized to a reference state Q_B^i and raised to the power M^i specific to each piece of equipment. Reference prices and quantities for various installations can be obtained from literature (e.g. [40]).

If more detailed information on the process conditions are available, they should also find their way into the cost estimation. Aside from the mere size of the equipment the process conditions will also influence the expected (and actual) cost. The predominant factors to that respect are pressure, temperature, corrosiveness and reactive activity, which will require single units to be manufactured from more resistant materials. Knowledge of a specific category for a piece of equipment to be installed will also lead to refined estimates. For example an plate-fin heat exchanger might be more expensive than a tubular model with the same heat-exchange area. In order to account for all those effect a form factor f_F can be applied to the equipment cost

$$C_E^i = C_B^i \left(\frac{Q_E^i}{Q_B^i} \right)^{M^i} f_F^i = C_B^i \left(\frac{Q_E^i}{Q_B^i} \right)^{M^i} \underbrace{\left(1 + f_C^i + f_M^i + f_P^i + f_T^i\right)}_{=f_F^i} . \tag{3.4}$$

Where f_F denotes the form factor, f_C corrects for design complexity, f_M for material selection, f_P adjusts for extreme pressures and f_T for temperature.

As in the previous section all reference prices need to be scaled for the temporal price development. Again the aforementioned indices are used. Furthermore can the prices be corrected for regional differences in price structure. Once more correction factors to prices in an reference region in the world (e.g. USA) are employed [36].

In addition to the purchased cost, the costs for installing the process equipment have an significant effect on the total needed investment of the process. These installation costs include:

- Installations costs
- Piping ,valves and electrical wiring
- Control system
- Structures and foundations
- Insulation and fire proofing
- Labour fees

To incorporate those additional costs, again correction factors to the main equipment price are used. Depending on the status of the information available they can be expressed as one unified factor or broken down to each specific category. One however needs to bear in mind, that costs for piping and valves – pieces of equipment in direct contact with process media – will be affected by the process conditions in a similar way as the actual equipment, whereas the other categories are more likely to remain unchanged. Thus attention needs to be paid, in which fashion the factors will be applied.

A word should be said about the cost for the control system. Most obtainable data will most likely refer to a decentralized control system, as it has been in use for many years. With ever more powerful computers a centralized approach, namely model predictive control (MPC) is becoming more relevant. As the structure for such a control system may vary significantly from the common designs, the cost factors may as well.

Services

The utility investments and off-site investments are often referred to as services. Therein included are all measures necessary to supply the process with the media consumed during operation. This includes but is not necessarily limited to generation and distribution of energy, steam and process gases. The utility investments in this context refer to all investments within the greater production site but out of the battery limits of the specific process. Off-site investments contain everything not contained in the site such as roads, power cables, communication systems or waste disposal. All these costs are expressed as fractions of the equipment cost at moderate temperature and pressure. This means, when applying these fractions, the factors f_M, f_P and f_T should not be considered at this point.

Once again in early design stages one has to resort to factors derived for statistical data, to calculate the cost of raw materials, energy and support media such as lubricants, heat or catalysts. If more detailed information on process streams is available the approach should be refined.

The cost of raw materials C_{RM} can then be calculated if the material streams of individual raw materials m_i as well as their specific cost are known.

$$C_{RM} = \left(\sum_{i}^{N_{RM}} \dot{m}_i \cdot C_{RM}^{i} \right) \cdot t_{op}. \tag{3.5}$$

Much in the same way the cost for energy can be approximated. As for the raw materials, this is once more done for each individual process unit, rather then for the process as a whole. Hence with the needed energy for equipment i with respect to energy carrier j e_{ij} along with the price for energy carrier j C_{EC}^{j} the total energy cost C_{EC} can be assessed

$$C_{EC} = \left(\sum_{i}^{N_E} \sum_{j}^{N_{EC}} \dot{e}_{ij} \cdot C_{EC}^{i} \right) \cdot t_{op}. \tag{3.6}$$

All cost related to utilities consumed during the operation of the process and not any eventual down time are calculated using the operating time t_{op}

Working capital

The working capital includes all investments necessary for process operations. This means raw materials, payroll, extended credit to customers and so on. In contrast to all other costs the working capital can partially be retrieved when the process ceases operations. How different types of cash flows, extended or owed credit should be handled will be disused in sec. 3.2. In addition to the cost of raw materials needed during process operations, which generate a product stream, raw materials are also needed to fill all vessels, reactors, columns and piping that make up the process. The cost of these should be considered as investment and not as operation cost [10], since more or less the same amount will remain bound until the process ceases operations and it can (partially) be retrieved.

$$C_{FILL} = \sum_{i}^{N_{RM}} V_i \cdot C_{RM}^{i}. \tag{3.7}$$

Total investment

When all contributions to the total investment are considered an estimate for the total price of the process can be calculated

$$C_P = \sum_{i}^{N_E} \left[C_B^i \left(\frac{Q^i}{Q_B^i} \right)^{M^i} \left(f_F \cdot f_{PIPE} + \sum_j f_j \right) \right] + C_{RM} + C_{EC} + C_{FILL} \tag{3.8}$$

It should be emphasized that in early design stages these calculations will at best yield an order of magnitude estimate for the expected cost of implementing a chemical process. Most literature sources give an accuracy of $\pm 30\%$ [36]. As the project progresses more and more information becomes available an a more accurate estimate can be prepared. The most refined ones rely on actual proposals from prospective manufacturers and suppliers.

3.2 Investment criteria

The total cost of a project is a very important measure to decide whether to embark on a certain endeavor. However in a complex financial system it cannot be taken as the sole factor to compare investment alternatives. Different other indices are used to measure the attractiveness or feasibility of an investment. One main distinction can be made between different measurements. Those that work with averaged cash flows and consider the project as a singe time period (sec. 3.2.1) and models that take into account cash flows made at different points in time – so called multi-period models (sec. 3.2.2). Some examples for both types of indices are the subject of the rest of this section.

3.2.1 Single period estimation methods

Among the most prominent single period methods are the payout time (POT) and the return on investment (ROI) which will be discussed in this section.

Payout time

Payout or amortization time is the time necessary to earn the total investment of the process. It is also often referred to as the break even point. A profitable venture will from that point on begin to make money. A shorter payback time can be considered a measure for an more attractive investment.

$$POT = \frac{\text{capital expenditure}}{\text{incoming cash flow / period}} \tag{3.9}$$

However many aspects especially in potential profits are not included here.

Return on investment

The return on investment is defined as

$$ROI = \frac{\text{average return / period}}{\text{capital expenditure}} \cdot 100\%. \tag{3.10}$$

It denotes the equivalent to an interest rate if the earned interest is not reinvested such that the same investment is considered in every period. The average return is calculated form the expected returns over certain duration of time. The time considered might either be the total life-cycle of the process or the expected write-off time. As capital expenditure most likely the total investment will be used. However it might give a more precise picture if write-off or the time of individual payments is considered when evaluating the capital expenditure.

3.2.2 Multi period estimation methods

As discussed earlier, when using only averaged values and considering only one time period, a distorted picture of the financial situation will evolve. The sources of the money to be invested play a critical

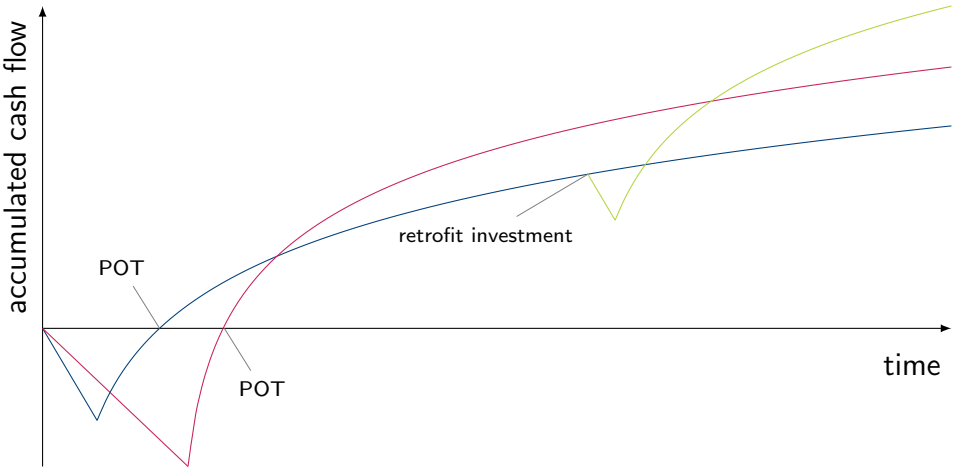

Figure 3.1: Accumulated cash flows over project life-cycle.[31]

role in the evaluation process. Cash reserves, loans, preferred stock or other financial instruments are all conceivable sources for investment capital. Especially for large scale projects often a mixture of many different sources is used to allocate all necessary funds.

A generic structure of the cash-flows during the life-cycle of a given project is shown in fig. 3.1. When the project commences no revenue is generated and only investments are made. As process operations begin revenue is generated and the slope of the accumulated cash flow curve switches to an upward directions – assuming the project is profitable. As time progresses the produced product might reduce in value through competitors entering the market or other factors. When the curve intersects the abscissa the project investment is earned and the break even point is reached. The two investment alternatives highlight that the amount of initial investment will affect the expected revenue. As more information is gathered during operations, opportunities may arise to optimize the process and leverage so far dormant potentials. These so called retrofit investments would ideally lead to an improved cash flow structure as indicated by the green line.

Before further investigating multi-period models some basic concepts of financial mathematics and the treatment of interest should be reviewed. When investing the capital C_0 at compounded interest for n years at a rate of i %, the compound amount will yield

$$C_n = C_0 \cdot q^n. \tag{3.11}$$

Where q denotes the interest factor

$$q = 1 + \frac{i}{100}. \tag{3.12}$$

On the other hand the current value of an investment that will yield C_n in n years can be calculated by

$$C_0 = C_n \cdot q^{-n} \tag{3.13}$$

The above considerations always assume a single payment at the beginning or end of the entire period. Annuities however are usually in several trances with regular payments to be made or received at

predefined instances. Assuming those payments are of equal size a, the final value can be computed by

$$C_n = a \cdot q^{\alpha} \cdot \frac{q^n - 1}{q - 1}, \tag{3.14}$$

while the current value of an annuity yields

$$C_0 = a \cdot q^{\alpha - n} \cdot \frac{q^n - 1}{q - 1}, \tag{3.15}$$

The factor α in the previous equations denotes whether payments are made at the beginning of a period ($\alpha = 1$ or at the end ($\alpha = 0$)

Given those basic considerations, multi-period model can be discussed. Here not only different alternatives can be compared, but also the profitability in comparison with investments in financial products can be assessed.

Net present value

The net present value (NPV) describes the amount of money to be invested if all cash flows – incoming and outgoing – are discounted to the project start ($t = 0$). The present value of all expenses is then

$$C_{0e} = e_0 + e_1 \cdot q^{-1} + \cdots + e_n \cdot q^{-n} = \sum_i^n e_i \cdot q^{-i}. \tag{3.16}$$

Here it is given that all expenses are paid at the beginning of each period, as it is the most common case. If revenues r_i are realized then as well an equivalent formula would be attained. In most cases revenues will come in at the end of a period in which case the present value becomes

$$C_{0r} = r_0 \cdot q^{-1} + r_1 \cdot q^{-2} + \cdots + r_n \cdot q^{-(n+1)} = \sum_i^n r_i \cdot q^{-(i+1)}. \tag{3.17}$$

The NPV of a project is then derived from the present values of all expenses and revenues

$$NPV = C_{0r} - C_{0e}. \tag{3.18}$$

For any project to be considered as investment alternative the present value needs to be positive since otherwise the investment would yield losses.

Discounted cash flow rate of return

The formula for the discounted cash flow rate of return is very similar to the one for a net present value. The difference is, that rather than computing the net present value with given interest rates, the present value is set to zero and the resulting interest rate its then calculated. Other than with

the previous methods no analytical solution can be presented but rather an iterative approach to find a solution to

$$0 = \sum_{i}^{n} (r_i - e_i) \cdot q^{-i}. \tag{3.19}$$

Here its was assumed that all payments – incoming and outgoing – are made at the beginning of a period. The only variable is the interest rate which is included in the interest factors q. This method gives the interest rate which would be necessary to earn all time dependent expenses within n years. In this case a higher $DCFRR$ indicates a more attractive investment.

Annuity method

Within the annuity method two different annuities are calculated and then compared. First the annuity a of an investment of C_0 at market conditions is of interest.

$$a = C_0 \cdot \frac{q^{n-\alpha}(q-1)}{q^n - 1} \tag{3.20}$$

This annuity is the amount that could be paid out each period if C_0 is invested, compound interest is considered and all funds are used up at the end of n years.

This is then compared to the annuity of the considered project

$$a_P = \sum_{i}^{n} (r_i - e_i) \cdot q^{-i} \cdot \frac{q^{n-\alpha}(q-1)}{q^n - 1}. \tag{3.21}$$

Only if $a_P > a$ is the project more profitable than simply investing the required capital in a financial product.

Interest Rates

With all the presented models it was implicitly assumed that interest rates for debit and credit are equal. The reality however is much different. It will therefore be prudent to use different rates of interest for each case. The basic calculations however remain unchanged. Especially the interest rate that can be earned when investing a certain amount will need to be estimated. As certain products with a know ROI will not necessarily be the most attractive options on the capital market. Thus in many companies there is an internal value given for this interest rate, which is calculated from historical data.

3.3 Economic process model

As discussed earlier economic consideration play a major role in process design. In order to account for the process economics the cost of the process to be implemented needs to be estimated at the

design level. However as limited information is available estimation methods have to be employed. In sec. 3.1 the general approach for cost estimation of process equipment was introduced, where a specific value such as heat-exchange area or vessel size is used to approximate equipment cost. However for more specific units extended models are available, where statistical data is employed to yield a more realistic fit to cost data. The cost functions and correction factors presented in this chapter are, if not stated otherwise, taken from [40]. Also unless otherwise stated the unit cost is given for the year 2006 ($CE = 500$).

3.3.1 Destillation column

The cost of a given distillation column C_{column} is comprised of three main parts, the cost for the vessel or tower itself C_{tower}, the cost for platforms, ladders, manholes, and nozzles C_{platform} and the cost for the internals $C_{\text{internals}}$

$$C_{\text{column}} = C_{\text{tower}} + C_{\text{platform}} + C_{\text{internals}}. \tag{3.22}$$

The determining factors for the cost of a tower are the construction material and the weight of the vessel. The material is considered by multiplying a base cost by a material factor f_M. Thus the cost for the tower can be approximated by

$$C_{tower} = f_M \cdot \exp\left[7.2756 + 0.18255 \cdot \ln(W_{tower}) + 0.02297 \cdot (\ln(W_{tower}))^2\right], \quad 9000 \leq W_{tower} \leq 2.5 \cdot 10^6. \tag{3.23}$$

In this correlation the weight W is measured in pounds ($[lbs]$)

For the support structures the following equation has bee presented

$$C_{\text{platform}} = 300.9 \cdot (d_{\text{column}})^{0.63316} \cdot (l_{\text{column}})^{0.80161}, \tag{3.24}$$

where both the diameter d_{column} and length l_{column} are measured in feet ($[ft]$).

The weight of the column is attained by calculation its volume and multiplying it by the mass density of the construction material $\tilde{\varrho}$

$$W_{\text{column}} = \pi(d_{\text{column}} + t_s)(l_{\text{column}} + 0.8 \cdot d_{\text{column}})t_s \cdot \tilde{\varrho}. \tag{3.25}$$

It needs to be noted, that in this formula, all measurements have to be adjusted to the measurement of the density. Newly appearing is the shell thickness t_s of the tower. In order to compute this, several aspects can be considered.

The ASME pressure vessel code formula is used to compute the minimum thickness due to the design pressure p_D of a tower

$$t_p = \frac{p_D\, d_{\text{column}}}{2\,S\,E - 1.2 p_D}, \tag{3.26}$$

where S denotes the maximum allowable stress and E the fractional weld efficiency.

The design pressure is computed from the operating pressure p_O

$$p_D = \max\left\{10, \exp\left[0.60600 + 0.91615 \cdot \ln(p_O) + 0.0015655 \cdot (\ln(p_O))^2\right]\right\}, \tag{3.27}$$

It should be pointed out the the pressures in the previous equation are measured in pound per square inch gauge ($[psig]$).

In addition to the thickness due to pressure, it should be considered – especially for tall vessels – that the vessel might have to withstand external forces such as strong winds or earthquakes. To account for external effects a security addition t_w to the pressure thickness can be computed

$$t_w = \frac{0.22(d_{\text{column}} + 18)l_{\text{column}}^2}{S d_{\text{column}}}. \tag{3.28}$$

Therefor the total shell thickness amounts to

$$t_s = t_p + t_w. \tag{3.29}$$

In the previous equations the column diameter and length have frequently been used, however no mention has been made as to how to attain these values. While for a given design these values will be fixed, in the context of an optimization they need to be considered as decision variables. These decisions are closely linked to the choice of column internals. In case of the column height the procedure is very similar for columns with trays and structured packings. In case of the diameter however a clear distinction has to be made. This is due to the fact, that a decision regarding the diameter will have to ensure feasible column operations, which means it will have to be large enough to avoid flooding within the column. Consequently the procedures for determining height and diameter will be dealt with separately for each type of internals.

Trays

For a trayed column the height can be determined from the number of stages n_S used multiplied by the plate spacing h_{plate}. In addition however it needs to be ensured, that control of the columns is still possible. At the sump of the tower liquid will accumulate during operations. While in an ideal case the liquid level would be constant, that cannot be assumed. Regularly there are three different liquid levels defined in a column. The high level (HLL), normal level (NLL) and the low level (LLL). These levels are defined such that it sufficient time for the liquid to reach these levels ($t_{min}^{HLL}, t_{min}^{NLL}, t_{min}^{LLL}$) , if no liquid id withdrawn anymore, or no liquid comes down from the column. Furthermore the times for reaching the reboiler inlet and the lowest plat will ne necessary. What duration to reach those levels will be sufficient needs to be decided by a control engineer.

With these times and heights the height of the tower can be expressed as

$$l_{\text{column}} = n_S \cdot h_{\text{plate}} + \left(\sum_i t_{min}^i H^i\right) \cdot \frac{L_{n_S}}{A_{\text{column}} \varrho^L}. \tag{3.30}$$

This leaves the diameter to be determined. The most important factor to that regard is the vapour velocity within the tower. It is to be chosen such that no flooding or entrainment will occur. The following equation to compute these operation boundaries are taken from [27].

First the fractional entrainment factor ent_j for 80% flooding at each stage j needs to be calculated

$$ent_j = 2.24 \cdot 10^{-3} \cdot 2.377 \exp\left[-9.394 \cdot FLV_j^{0.314}\right], \qquad j = 1 \dots n_S. \tag{3.31}$$

Therein the Sherwood flow parameter FLV_j is used

$$FLV_j = \frac{\tilde{L}_j}{\tilde{V}_j} \cdot \sqrt{\frac{\tilde{\varrho}_j^V}{\tilde{\varrho}_j^L}}, \qquad j = 1 \dots n_S, \tag{3.32}$$

$$v_j^{flood} = 60 \cdot \left(\frac{\sigma_j^L}{20}\right)^{0.2} \cdot K1_j \cdot \sqrt{\frac{\tilde{\varrho}_j^L - \tilde{\varrho}_j^V}{\tilde{\varrho}_j^V}}, \qquad j = 1 \dots n_S, \tag{3.33}$$

$$K1_j = 1.05 \cdot 10^{-2} + 0.1496 \cdot h_{\text{plate}}^{0.755} \cdot \exp\left[-1.463 \cdot FLV_j^{0.842}\right], \qquad j = 1 \dots n_S. \tag{3.34}$$

With those values the minimum required column area for each stage A_j^{min} can be calculated

$$A_j^{min} = \frac{V_j}{\Psi_{flood} \varrho_j^V v_j^{flood}}, \qquad j = 1 \dots n_S, \tag{3.35}$$

where Ψ_{flood} is a design parameter which determines the degree of flooding allowed and will usually have a value around 0.8.

Structured packings

The calculation of the column height is equivalent to the trayed case, with the one difference, that rather than using the plate spacing as the height for each stage a value called height equivalent to to theoretical plate ($HETP$) ist used. In terms of the column diameter the flooding velocity is determined by the flooding pressure drop as calculated in sec. 4.2.1.

3.3.2 Centrifugal pump

Pumps are among the most common units of process equipment. While there are several different kinds of pumps that can be used, the centrifugal pump is one of the most popular choices and denotes a very likely choice for the process conditions considered in this application. Hence other pump types will not be considered at this point.

Pump In terms of operations pumps are best described by the volumetric flow transported Q as well as the pump head H, the hight that needs to be overcome. Data taken from the company Mosanto was used to correlate the pump cost to a specific value

$$S = Q\sqrt{H}. \tag{3.36}$$

stages	rpm	case-split	flow ([gpm])	head ([ft])	pow ([Hp])	f_T
1	3600	VSC	50 - 900	50 - 400	75	1.00
1	1800	VSC	50 - 3500	50 - 200	200	1.50
1	3600	HSC	100 - 1500	100 - 450	150	1.70
1	1800	HSC	250 - 5000	50 - 500	250	2.00
2	3600	HSC	50 - 1100	300 - 1100	250	2.70
2+	3600	HSC	100 - 1500	650 - 3200	1450	8.90

(a) type factors.

material	f_m
cast iron	1.00
ductile iron	1.15
cast steel	1.35
bronze	1.90
stainless teel	2.00
Hastelloy C	2.95
monel	3.30
nickel	3.50
titanium	9.70

(b) material factors.

Table 3.2: Pump cost factors [40].

As a reference unit the base price C_B is estimated for a cast iron single-stage vertically split case at 3600 rpm

$$C_B = \exp\left\{9.7171 - 0.6019 \cdot \ln[S] + 0.0519(\ln[S])^2\right\}, \qquad 400 \leq S \leq 100000. \tag{3.37}$$

The most influential scaling factors for the pump price are the material, which is accounted for in the material factor f_m, as well as the rotation, case split orientation (horizontal and vertical), the number of stages, covered flow rate range, pump head range and maximum motor power, which are all agglomerated in the type factor f_T. Values for these factors are given in tab. 3.2a and tab. 3.2b.

Electric motor Separately from the pump itself the motor to drive the compression is considered. While the volumetric flow and the pump head certainly are valid choices to correlate motors for pumps especially, the power consumption is a more general specific value

$$P_C = \frac{P_T}{\eta_P \eta_M} = \frac{P_B}{\eta_M} \tag{3.38}$$

It can be calculated from the theoretic power of the pump P_T and the efficiencies η_P η_M. While an estimate for the expected power consumption might be already available at rather early design stages, the efficiencies will have to be correlated as well if resorting to average values is considered too coarse. Those correlations rely on the volumetric flow in gallons per minute ([gpm]) and the brake horse power $P_B = \frac{P_T}{\eta_P}$.

$$\eta_P = -0.316 + 0.24015 \cdot \ln[Q] - 0.01199 \cdot (\ln[Q])^2 \qquad 50 \leq Q \leq 5000 \tag{3.39}$$

$$\eta_M = 0.80 + 0.0319 \cdot \ln[P_B] - 0.00182 \cdot (\ln[P_B])^2 \qquad 1 \leq P_B \leq 1500 \tag{3.40}$$

After having calculated the power which the motor needs to supply its base cost of an open, drip-proof enclosed motor at 3600 rpm can be approximated by

$$\begin{aligned} C_B = \exp\big\{&5.8259 + 0.13141 \cdot \ln[P_C] + 0.053255 \cdot (\ln[P_C])^2 \\ &+ 0.028628 \cdot (\ln[P_C])^3 - 0.0035549 \cdot (\ln[P_C])^4\big\} \qquad 1 \leq P_C \leq 700 \end{aligned} \tag{3.41}$$

To adjust the cost for different types of electric motors the type factors from tab. 3.3

type motor enclosure	3600 rpm	1800 rpm
open, drip-proof enclosure, 1 to 700 Hp	1.0	0.9
totally enclosed, fan-cooled, 1 to 250 Hp	1.4	1.3
explosion-proof encosure, 1 to 250 Hp	1.8	1.7

Table 3.3: Type factors for different motor types.

Compressor

The cost of compressors is correlated with their respective power consumption measured in horsepower. Although not the most efficient type of compressor, centrifugal compressors are very popular in the process industry, as they are easily controlled an deliver a very steady flow. However as different types might be employed as well base cost correlations for centrifugal, reciprocation and screw compressors are given.

Centrifugal compressor

$$C_B = \exp\left\{7.5800 + 0.80 \cdot (\ln[P_C])\right\} \qquad 200 \leq P_C \leq 30000 \tag{3.42}$$

Reciprocating compressor

$$C_B = \exp\left\{7.9661 + 0.80 \cdot (\ln[P_C])\right\} \qquad 200 \leq P_C \leq 20000 \tag{3.43}$$

Screw compressor

$$C_B = \exp\left\{8.1238 + 0.7243 \cdot (\ln[P_C])\right\} \qquad 200 \leq P_C \leq 750 \tag{3.44}$$

Again as with most other equipment types correction factors are used to adjust for different realization of this piece of equipment. Here type of motor as well as the construction material have the biggest effects on the unit price and are explicitly considered.

$$C_p = f_D \, f_M \, C_B \tag{3.45}$$

The alternatives to the electric motor ($f_D = 1.0$) are a steam turbine ($f_D = 1.15$) or a gas turbine ($f_D = 1.25$). It should however be noted that aside from being the cheapest choice, the electric motor is also the most efficient. Thus the turbines are mostly considered, when process steam or combustion gas is easily available, such that the drawbacks might be eliminated by not having to supply the electric energy for the electric motor. In terms of construction material all base costs are for cast iron or carbon steel. Some appliances may require more resistant and also more expensive materials such as stainless steel ($f_M = 2.5$) or an nickel alloy ($f_M = 5.0$).

Reboiler / condenser

Reboiler and condenser can be characterized as heat exchangers, and be handled in the same way, as the main difference is weather heat is transferred to or from the process stream. In that sense they must be distinguished when considering the operating cost, as the cost for hot or cold auxiliary streams might differ significantly. As customary for heat exchangers the specific quantity for cost correlations is the necessary heat exchange area A measured in ft.

Again the construction material as well as the operating conditions have an effect on the final cost

$$C_p = f_P \, f_M \, C_B. \tag{3.46}$$

The correction for pressures f_P takes into account the operating pressure P_o and is computed by

$$f_P = 0.8510 + 0.1292 P_o + 0.0198 * P_o^2. \tag{3.47}$$

The material correction factor f_M

$$f_M = \tag{3.48}$$

Shell and tube heat exchanger

$$C_B = \exp\left\{11.667 - 0.8709 \cdot (\ln[A]) + 0.09005 \cdot (\ln[A])^2\right\} \tag{3.49}$$

Double pipe

$$C_B = \exp\left\{7.146 + 0.1600 \cdot (\ln[A])\right\} \tag{3.50}$$

4 Mathematical process model

This chapter will illustrate different process units and their mathematical representation. As depicted in fig. 4.1 three of the major tasks within the cryogenic air separation process will be regarded, when formulating the process. These are the compression of ambient air, heat exchange with product streams and the separation of streams. While those different stages are highly interdependent they will be discussed separately and mathematical models for the various process units contained in each stage will be presented.

The first section (sec. 4.1) deals with a steady state version of the process model. Especially for steady state models the issue of initializing the variables in such a way that the solver can converge to a solution becomes crucial. With that in mind the strategies developed to initialize in particular the distillation columns will also be elaborated upon. The second section (sec. 4.2) is devoted to a dynamic version of the models for some process units. In addition to the models themselves several aspects which arise when considering process dynamics, will also be part of that section. The models used to determine thermodynamic properties of process streams are briefly introduced in sec. 4.3. However these equations were not manually implemented are available from external routines through a foreign object interface within gPROMS®. All other presented models have been implemented in the equation based process simulator. Certain aspects arising when implementing the models will be discussed in the last section of this chapter sec. 4.4.

4.1 Steady - state unit models

Most continuous processes are designed to operate at steady-state. If so, no temporal gradients are present during process operations. A detailed knowledge about steady-state process behaviour is therefore essential to designing processes at a certain operating point.

In this section several models required for simulating the ASU process at steady-state operations are presented. All major tasks highlighted in fig. 4.1 will be considered here.

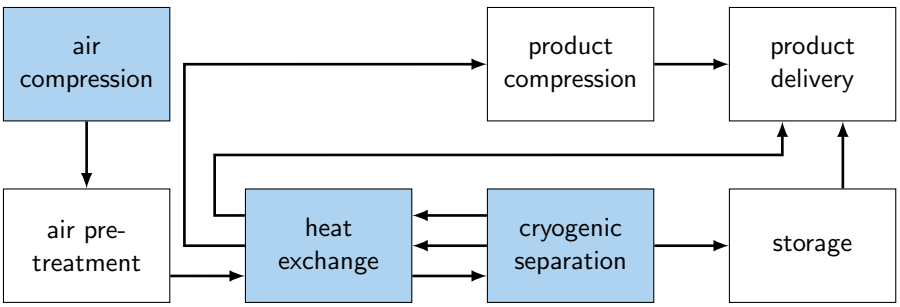

Figure 4.1: simplified cryogenic air separation process.

4.1.1 Separation

The separation step within the process occurs within a double effect distillation column. Distillation columns are among the most widely studied pieces of process equipment. While much has been accomplished, the robust simulation poses great challenges to this day. In the context of cryogenic air separation the associated mixture displays only moderate non-idealities and furthermore is a zeotropic one. The main complexity however is due to the strong interdependencies of the different columns arising from thermal and material coupling within the process.

In this section first the mathematical formulation for a general steady-state distillation column model, which has been developed as a multi-purpose, easily applicable model for the process simulator gPROMS®, will be presented (sec. 4.1.1). As one of the specialties of the ASU process, an integrated condenser and reboiler unit is employed. Especially for the dynamic case, explicitly considering this fact this can be used for model simplifications. In order to have an equivalent set of models, a steady-state version is presented here as well (sec. 4.1.1).

Distillation column model

The core equations describing the operation of any distillation column, or more general vapour liquid contacting device, are often referred to as the MESH equations [21]. The acronym MESH stands for material, equilibrium, summation and enthalpy (often represented by the symbol H). These equations, although rather plain at first glimpse, form a set of highly non-linear, highly coupled equations. The solutions of which poses a non-trivial task for current solution algorithms, whose success is highly dependent on the quality of initial estimates for the involved variables. Therefore a strategy used for the automated generation of such guesses will be described as well.

The model presented here is not only to be used for the simulation of a given process, but rather for optimization purposes as well. While several of the decision variables associated with the process can be optimized from a generic set of equations, others need further consideration. The optimization decisions which add the greatest complexity for distillation columns are the locations for feeds and side draws, as well the number of trays for a given separation task. Part of the added complexity is the introduction of integer decisions into the model and and the associated need for a super structure which includes all process alternatives to be considered.

The starting point for the model development is a single separation stage within the column with all possible material and energy streams entering and leaving the stage. Fig. 4.2a shows the superstructure to be used for the complete column, while fig. 4.2b shows a super structure for a single separation stage.

If not stated otherwise, all equations presented in this section apply to all separation stages. In order to improve readability the indices denoting a stage are sometimes omitted, if not essential for the meaning of a given equation. throughout the description of the models and the thesis the number of stages in a column section will be denoted by n_S, while n_C, n_F, n_{SV} and n_{SL} represent the total number of components, feeds, vapour and liquid side draws respectively.

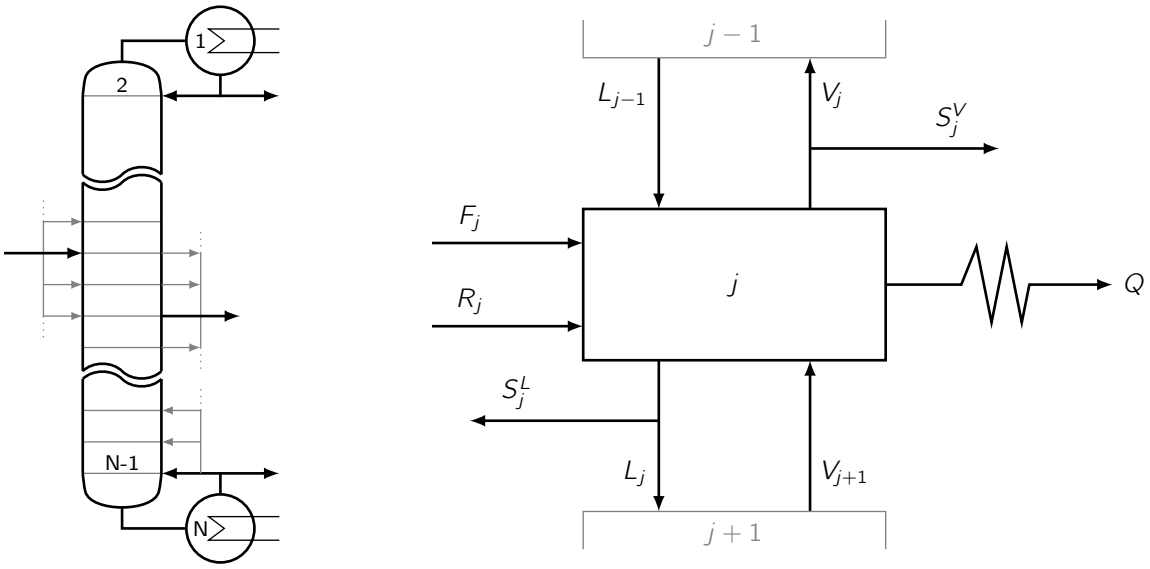

(a) column super structure.

(b) stage super structure.

Figure 4.2: superstructures for column and column stages.

Material balances in their most general form for an inner column stage can be written as

$$0 = \left(V_j + S_j^V\right) \cdot y_{i,j} + \left(L_j + S_j^L\right) \cdot x_{i,j} - V_{j+1} \cdot y_{i,j+1} - L_{j-1} \cdot x_{i,j-1} - F_j \cdot z_{i,j}, \quad i = 1 \ldots n_C \quad j = 1 \ldots n_S. \tag{4.1}$$

A certain amount of the liquid or vapour leaving a stage can be withdrawn from the column by means of the vapour S_j^V and liquid S_j^L side draw streams. During model development it was observed, that when a specification was made on given side-draw, convergence was sometimes hindered. This behaviour could be improved by specifying a dimensionless side-draw,

$$s_j^V = \frac{S_j^V}{V_j}, \qquad j = 1 \ldots n_S, \tag{4.2}$$

$$s_j^L = \frac{S_j^L}{V_j}, \qquad j = 1 \ldots n_S, \tag{4.3}$$

rather than an actual stream. It should be noted, that this technically introduces further non-linearities into the material balances. As it is difficult, to guess the dimensionless side draw for a desired side draw flowrate, the specification can be replaced by a specification on the flowrate, once model initialization has been achieved.

By considering these dimensionless side-draws the material balance can be rewritten as

$$0 = \left(1 + s_j^V\right) \cdot V_j \cdot y_{i,j} + \left(1 + s_j^L\right) \cdot L_j \cdot x_{i,j} - V_{j+1} \cdot y_{i,j+1} - L_{j-1} \cdot x_{i,j-1} - F_j \cdot z_{i,j}, \quad i = 1 \ldots n_C \quad j = 1 \ldots n_S. \tag{4.4}$$

As the model is also to be used for optimization of structural decisions, further extensions are necessary. To accommodate that need, new variables are introduced. Particularly split variables ζ as employed by [11] are introduced for feeds, vapour and liquid side draws and the reflux location. As

the feeds are and side draws are to be fed or taken from a single stage, the split variables must assume integer values of either one or zero. Furthermore those decisions are *exclusive or* type decisions, hence

$$1 = \sum \zeta. \tag{4.5}$$

In order to optimize the number of stages several superstructures are possible. One can optimize the reboiler reflux location and condenser reflux location or each single one along with the feed and side draw locations. The number of stages is then changed as all stages between condenser or reboiler reflux are effectively rendered inactive. The solution of the mass and energy balances for each inactive stage becomes trivial as only one single vapour or liquid stream enters and exits the stage.

While the choice if condenser and / or reboiler reflux is optimized is somewhat arbitrary, some studies have shown [15] that the strategy of optimizing only feed location and reboiler reflux location possesses some numerical advantages in terms of performance of the solution algorithm. However this observation might be specific to the particular solver used. Furthermore, as will be seen later, there are certain situations where optimizing either reboiler or condenser reflux is beneficial in terms of problem formulation. The developed model therefore offers capabilities to choose, whether the top or bottom reflux is variable. Either reflux will be represented by the generic variable R.

With the newly introduced split variables for the feed ζ_{ij}^{F} as well as the reboiler reflux ζ_{j}^{R} and the liquid ζ_{ij}^{SL} and vapour ζ_{ij}^{SV} side draws, the material balances can be written as

$$\begin{aligned} 0 = \left(1 + s_j^V\right) \cdot V_j \cdot y_{i,j} + \left(1 + s_j^L\right) \cdot L_j \cdot x_{i,j} - V_{j+1} \cdot y_{i,j+1} \\ - L_{j-1} \cdot x_{i,j-1} - \sum_{k=1}^{n_F} \zeta_{kj}^{F} \cdot F_j \cdot z_{i,j} - \zeta_j^R \cdot R \cdot z_R, \\ i = 1 \ldots C, \quad j = 1 \ldots n_S, \quad k = 1 \ldots n_F. \end{aligned} \tag{4.6}$$

Furthermore to be able to optimize side draws, the stripping factors have to be reformulated accordingly

$$s_j^V = \frac{\sum_{i=1}^{n_{SV}} \zeta_{ij}^{SV} S_j^V}{V_j}, \qquad j = 1 \ldots n_S, \quad i = 1 \ldots n_{SV}, \tag{4.7}$$

$$s_j^L = \frac{\sum_{i=1}^{n_{SL}} \zeta_{ij}^{SL} S_j^L}{L_j}, \qquad j = 1 \ldots n_S, \quad i = 1 \ldots n_{SL}. \tag{4.8}$$

Equilibrium between a vapour and liquid is achieved when the chemical potentials for each component in both pases are equal. This is commonly expressed by a equilibrium constant (K_i). With that the equilibrium equation can be written as

$$y_i^{eq} = K_i \cdot x_i, \qquad i = 1 \ldots n_C. \tag{4.9}$$

The requirement for equal chemical potentials can be expressed in terms of the vapour f_i^V and liquid f_i^L fugacities [2].

$$f_i^V = f_i^L, \qquad i = 1 \dots n_C. \tag{4.10}$$

These fugacities are calculated from the liquid activity coefficients γ_i, the pointing factor F_{Pi}, the reference vapour fugacity coefficient φ_i, the component saturation pressure p_i^S as well as the system pressure p along with the vapour and liquid molar fractions

$$\gamma_i \, F_{Pi} \, \varphi_i^0 \, p_i^S \, x_i = \varphi_i \, p \, y_i, \qquad i = 1 \dots n_C. \tag{4.11}$$

After simple rearrangement eq. (4.12) an expression for the equilibrium ratios can be derived

$$y_i^{eq} = \underbrace{\frac{\gamma_i \, F_{Pi} \, \varphi_i^0 \, p_i^S}{\varphi_i \, p}}_{K_i} x_i, \qquad i = 1 \dots n_C. \tag{4.12}$$

The equations to determine the quantities used when computing the equilibrium ratios are by themselves functions of temperature, pressure, and vapour as well as liquid molar fractions. They are further discussed in sec. 4.3. It therefore becomes evident that the equilibrium ratios are a major source for the non-linearities in the presented model.

When simulating a distillation process one might consider only equilibrium stages. This however will in most cases not reflect the true behaviour of a real stage as the time a vapour and liquid phase are in contact might not suffice to achieve equilibrium conditions. This can be accounted for by introduction of Murphee tray efficiencies [17]

$$\eta_{ij}^{eq} = \frac{y_{ij} - y_{ij+1}}{y_{ij}^{eq} - y_{ij+1}}, \qquad i = 1 \dots n_C \quad j = 1 \dots n_S. \tag{4.13}$$

While several models to approximate these efficiencies have been investigated, their predictions are most often rather poor [10] and their evaluation rather complex. Furthermore as indicated in the formula they might differ for different species involved. For this model however they are not computed separately, but rather supplied and assumed constant for all stages and components.

Enthalpy balances are again written considering the previously defined stripping factors and splitting variables

$$\begin{aligned} 0 = \left(1 + s_j^V\right) \cdot V_j \cdot h_j^V + \left(1 + s_j^L\right) \cdot L_j \cdot h_j^L - V_{j+1} \cdot h_{j+1}^V \\ - L_{j-1} \cdot h_{j-1}^L - \sum_{k=1}^{n_F} \zeta_{kj}^F \cdot F_k \cdot h_j^F - \zeta_j^R \cdot H_R - Q_j, \\ i = 1 \dots n_C, \quad j = 1 \dots n_S, \quad k = 1 \dots n_F. \end{aligned} \tag{4.14}$$

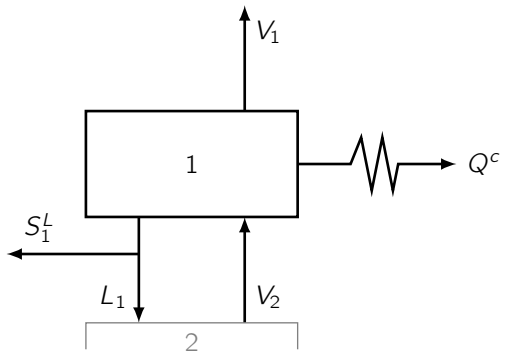

(a) condenser stage.

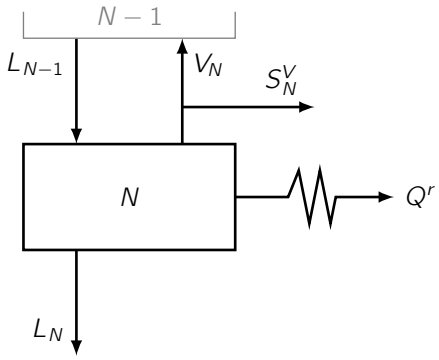

(b) reboiler stage.

Condenser and reboiler are modeled more or less as regular column stages. However they possess certain specialties that are explicitly considered in the column model. For one it is assumed that no feeds enter the condenser stage. Furthermore no vapour side stream is drawn from the condenser as well as no liquid side stream from the reboiler.

Additionally the condenser stage needs to examined a little further. In terms of operations several assumptions can be made for the condenser. In general one can distinguish a total, partial vapour and partial vapour liquid condenser. For the total condenser all vapour that enters the respective stage is condensed and only liquid product is drawn. The partial vapour condenser condenses only the vapour the which is to be fed back into the column and all product that is drawn is gaseous. The partial vapour liquid condenser denotes the most general case, where part of the incoming vapour is condensed and product is drawn from the vapour and liquid phase. The most important thing to consider in these different cases is, that while in both partial condensers a vapour liquid equilibrium takes place. Due to the absence of vapour the same does not hold for the total condenser. To accommodate that fact the MESH equations have to be adjusted [33]. While the material and energy balances remain unchanged the equilibrium equations have to be altered. First the vapour and liquid compositions are set equal for all but one component

$$x_{i1} = y_{i1} \qquad i = 1 \ldots C-1, \tag{4.15}$$

and the condenser temperature is determined by the bubble point equation

$$1 = \sum_i K_{i1}(T_1, p_1, x_1, y_1) \cdot x_{i1} \qquad i = 1 \ldots n_C. \tag{4.16}$$

When implementing the model in a process simulator it is sensible to consider, that due to the limited accuracy of computers the omitted component in eq. (4.15) needs to be a non-trace component in the condenser stage. The implemented model therefore has to specify such a component when a total condenser is chosen to avoid numerical difficulties.

In practice it is highly unlikely, that the exact amount of energy required to condensate all liquid will be drawn from the condenser. More likely, if all vapour is condensed, slightly more energy will be withdrawn and sub-cooled liquid will leave the condenser. Therefore the model includes the possibility to specify a degree of sub-cooling T^{sub} which will be considered when calculating bubble point temperature

$$1 = \sum_i K_{i1}(T_1 + T^{sub}, p_1, x_1, y_1) \cdot x_{i1} \qquad i = 1 \ldots n_C. \tag{4.17}$$

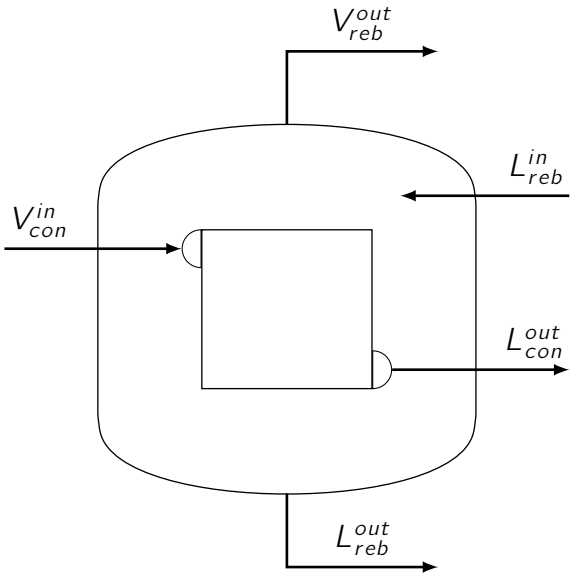

Figure 4.3: Integrated condenser & reboiler unit.

Pressure along the entire column is often specified in the steady-state case. However as it is inconvenient and unpractical to specify a pressure for each stage one might either specify a pressure at the top and bottom stage and assume a uniform pressure profile along the column, or specify either top p_1 or bottom pressure p_N along with a total pressure drop Δp, or a stage-wise one Δp_{stage}. However the issue is further complicated if one considers the case of optimization for number of trays. In that case several trays will become inactive. For those trays the mass and energy balances become trivial, as only liquid enters and exits these trays. (For the case employed here, where the reboiler reflux is being optimized). This also means, that from the last active tray down to the reboiler – if present – there should be a uniform profile. It is important to note, that if a uniform pressure profile from the lowest active stage downward is not enforced, the solver will have to compensate for slight changes in the equilibrium due to pressure variations with minimal vapour flow-rates. This is very undesirable, as it might lead to severe problems in the solver, or the calculation of other properties, dependent on these values. To account for this issue, the reboiler reflux split be employed to deactivate the pressure drop

$$p_i = p_{j-1} + \left(1 - \sum_{k=1}^{j-1} \zeta_k^R\right) \cdot \Delta p_{j-1} \qquad j = 1 \ldots n_S. \tag{4.18}$$

As an alternative to specifying the pressure, one might consider calculating the pressure drop form (semi)-empirical models. There a numerous correlations for different types of column internals. These correlations become particularly important if column dynamics are to be considered, as they form the connection between holdups and flow-rates within the column. Two different pressure drop models have been implemented, one for trayed columns and another one for structured packings. As they are closely tied to dynamics, they will be discussed in more detail in sec. 4.2.

Integrated condenser & reboiler

The integrated condenser reboiler unit is a peculiarity of the ASU process. The fact that condenser and reboiler are linked form the close coupling between both sections of the double effect column. This stems from the fact, that each change in the parameters and operation of this unit will reverberate through the entire process, as they will simultaneously affect boil-up ratio and reflux ratio of the column, both major operational parameters with great effect.

Therefore a separate model for this unit was developed, rather that simply establishing a couple between the the condenser and the reboiler in the case for two separately modeled column sections.

The reboiler side is modeled much like an equilibrium stage in the column, considering the entering and leaving streams as depicted in fig. 4.1.1. However in contrast to the equations supplied for a column section, no integer optimization terms will have to be considered. Furthermore no side draws, or separate feeds are recognized. With that the material balances are

$$0 = L_{reb}^{in} x_{i,reb}^{in} - L_{reb}^{out} x_i^{reb} - V_{reb}^{out} y_i^{reb}, \qquad i = 1 \dots n_C. \tag{4.19}$$

The energy balance taking into account the transferred energy (Q_{CR}) becomes therefore

$$0 = L_{reb}^{in} h_{reb}^{in} - L_{reb}^{out} h_{reb}^{L} - V_{reb}^{out} h_{reb}^{V} + Q_{CR}. \tag{4.20}$$

The equilibrium and summation equations are analogous to the ones presented for the column model. A pressure drop again is assigned with relation to the lowest column stage.

The condenser is modeled as a total condenser. The mass and component balances therefore become trivial

$$x_{i,con} = y_{i,con}^{in}, \qquad i = 1 \dots n_C, \tag{4.21}$$

$$V_{con}^{in} = L_{con}^{out}. \tag{4.22}$$

The temperature is set to the bubble temperature of the given mixture at an assigned pressure. The enthalpies of the entering and leaving stream can therefore be calculated from the given EOS. And the energy balance determines the transferred energy

$$0 = V_{con}^{in} h_{con}^{in} - L_{con}^{out} h_{con}^{L} - Q_{CR}. \tag{4.23}$$

4.1.2 Heat exchange

The issue of heat integration is essential to the economic performance of cryogenic air separation. Foremost one must consider the special column configuration used in the process. Since operation of the condenser in the low pressure section only becomes possible if the reboiler in the high pressure section functions as heat sink, no external utilities are supplied to either unit. Rather they are combined into a single heat exchange unit. Thus the absolute value of the reboiler energy must matched by the energy recovered from the condenser (see sec. 4.1.1). Furthermore the material streams entering the process can – and should – exchange heat with the process streams leaving it. The combined condenser & reboiler for the double effect column is assumed as a given heat exchange.

This makes sense insofar, as this is a necessity in terms of the actual physical implementation of the process units. Also the usage of the oxygen rich liquid from the HPC as coolant in the Argon condenser is assumed as fixed.

This leaves the process stream leaving the compression stage of the process as well as all product and waste streams leaving the process. All those streams are – for simulation purposes and also in some process implementations – fed into a single multi-stream heat exchange unit. In actual processes all heat exchange and much of the process operations take place in the so called "cold box". As such a heavily insulated area is referred to. This is done to minimize heat exchange with the surroundings. Therefore and for further reasons compact heat exchange units such as plate-fin multi-stream heat exchangers are favoured when dealing with cryogenic processes in general and the cryogenic air septation in particular.

Due to the importance of heat integration to the ASU process some thought should be given as to what modelling approach should be employed. Although the field of heat integration is one of the most intensively studied within process engineering, only a limited amount of approaches is available in open literature [19].

A very simple approach is to employ enthalpy and material balances around the entire unit.

$$0 = \sum_j \left(H_j^{in} - H_j^{out} \right), \tag{4.24}$$

$$0 = x_{ji}^{in} - x_{ji}^{out}, \tag{4.25}$$

$$0 = p_i^{in} - p_j^{out} - \Delta p_j, \tag{4.26}$$

$$0 = F_j^{in} - F_j^{out}. \tag{4.27}$$

Here all entering process streams are variable but determined by the respective model equations they are originating from. Hence all but one outlet stream temperature along with all pressure drops must be specified.

4.1.3 Compression & expansion

The issue of cooling the ambient air to process temperatures at around $90K$ is not an easy one. The main hindrance is, that a heat sink at this temperature level is not readily available. Lucky thermodynamics offer a different way to reach such temperatures. In order to do so, the ambient air first needs to be compressed and then expanded again. Cooling then occurs by either exploiting the *Joule-Thompson* effect or isentropic expansion. First a few comments are made about the compression stage, while afterwards the governing principles for cooling by expansion will be described.

Multi-stage compression

Compressors and expanders are among the most common process equipment. A multitude of processes utilizes them as primary or auxiliary units. In the context of cryogenic air separation the compression plays a major role, as it enables to reach temperatures needed for liquefying air and gases in general. As the compression of gases is always associated with a significant reduction in

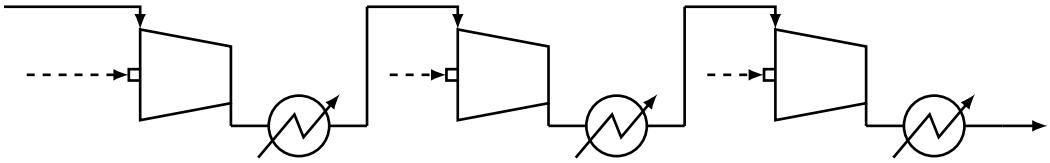

Figure 4.4: Multi-stage compression.

volume it requires large amounts of energy. Thus in addition to significantly contributing to the capital cost of the process the compression stage is responsible for the majority of the operating cost encountered in the ASU process.

The rigorous modeling of continuous flow machines in terms of unit operations poses great challenges. For specific units it may be undertaken by means of CFD simulations or employing characteristics diagrams, which require extensive experiments or can be obtained from the manufacturer. For the purposes of process design however a simpler approach with unit efficiencies is appropriate.

As a significant temperature increase goes along with the compression of air and in order to reduce the energy demand of the compression in general, it is beneficial, to use a multi stage compressor with inter-cooling stages as depicted in fig. 4.4. This yields a lower energy consumption as a single stage unit for the same compression ratio.

Subsequently the working equations for the compressor model used in the scope of this thesis are briefly summarized.

A trivial material and component balance around the compressor yields the outlet molar flow-rate F^{out} as well as the outlet overall composition z^{out}

$$0 = F^{in} - F^{out}, \tag{4.28}$$

$$0 = z_i^{in} - z_i^{out} \qquad i = 1 \dots n_C. \tag{4.29}$$

To calculate the mechanical work associated with the desired compression, first the isentropic case

$$S^{in} = S^{out} \tag{4.30}$$

is considered. With that the isentropic work W_S is calculated. Here the exit enthalpy in the isentropic case H_S^{out} is used.

$$W_S = F^{in} \cdot (H^{in} - H_S^{out}) \tag{4.31}$$

With the isentropic efficiency η^C, the actual work W and outlet enthalpy determined,

$$W \cdot \eta^C = W_S, W_S = F^{in} \cdot (H^{in} - H^{out}). \tag{4.32}$$

Finally the pressure drop over the unit needs to be considered

$$p^{out} = p^{in} + \Delta p. \tag{4.33}$$

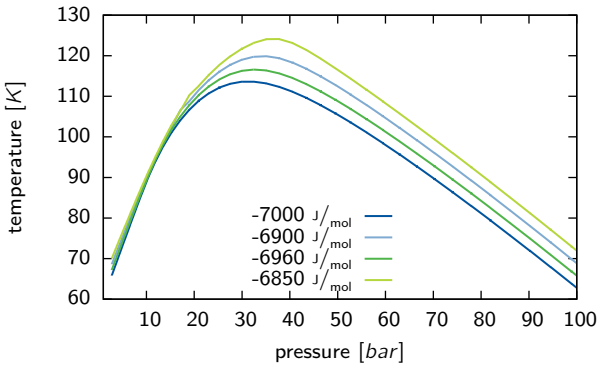

Figure 4.5: Isenthalpes computed by Peng-Robinson EOS.

Cooling by expansion

The liquefaction of gases requires temperatures well below ambient conditions. In order to attain such conditions one cannot utilize natural occurring coolants as they are not available at the required temperature level. Rather cooling effects that can occur during the expansion of gases are exploited. First we consider the expansion through an expansion valve or so called *Joule-Thompson* - valve. In an rather accurate approximation, expansion through a valve can approximated as an isenthalpic process ($h_1 = h_2$). To describe the change in temperature during isenthalpic expansion the *Joule-Thompson* coefficient

$$\mu_{JT} = \left(\frac{\partial T}{\partial p}\right)_h, \tag{4.34}$$

which denotes pressure derivative of the temperature at constant enthalpy can be considered. This can be transformed into

$$\mu_{JT} = \frac{1}{c_p}\left[T\left(\frac{\partial v}{\partial T}\right)_p - v\right] \tag{4.35}$$

If we employ the Peng-Robinson equation of state, which is appropriate for this mildly non-ideal system [2], we can plot the isenthalpes for ambient air ($x_{N_2} = 0.7812$, $x_{O_2} = 0.2095$, $x_{Ar} = 0.0093$) in a PT-diagramm (fig. 4.5). There we can see, that in certain ranges a decrease in pressure at constant enthalpy will result in an increase in temperature, while for other regions temperature decreases. It is interesting to mention that the non-idealities of a given gas give rise to this effect. For an ideal gas the temperature change at isenthalpic expansion would always be zero. Luckily for the cryogenic engineer real gases deviate from ideal behaviour especially at elevated pressures and low temperatures [3]. It is therefore important to give some consideration to the thermodynamic model used to describe the properties of the system in question, as the non-ideal properties need to be captured appropriately.

A different way of expanding a compressed gas, is by letting it produce work in an fluid kinetic machine. If one assumes an adiabatic devices and disregards irreversible effects, this process can be viewed as isentropic. Analogous to the isenthalpic case an isentropic expansion coefficient can be

defined

$$\mu_S = \left(\frac{\partial T}{\partial p}\right)_S = \frac{T}{c_p}\left(\frac{\partial v}{\partial T}\right)_p . \tag{4.36}$$

Here the derivative in the second form corresponds to the volumetric coefficient of thermal expansion β, which is always positive for gases, which in turn means, that an isentropic expansion will always result in an temperature decrease, whereas the isenthalpic expansion only led to a decrease for specific conditions. Furthermore an isentropic expansion over the same pressure range will always result in lower temperatures than an isenthalpic expansion. The reason that isentropic valves are most commonly used in liquefaction systems, is that those work producing machines cannot handle significant phase changes, which is after all the desired result of liquefaction.

Traditionally only the isenthalpic expansion had been used within the cryogenic air separation process, since – as mentioned before – the air needs to be liquefied in order to be fed into be distilled. However in modern process configurations the isentropic expansion is also considered to recover some of energy form the compression.

4.2 Dynamic unit models

The models presented in the previous section are suited to optimize the desired process operation. While models like that offer valuable insight into the operation of a process many aspects remain unclear. Questions of operability or stability of the process, or if a given steady state can actually be acquired in finite time are beyond the scope of steady state models. In order to supply answers to aforementioned questions, dynamic versions of the previously discussed unit models are needed. As the capture of dynamic effects requires a much higher level of detail, since mass and energy transport phenomena and hydrodynamics have to be considered, they also are more cumbersome to implement. While all aspects of the process carry great relevance for process operations, the concern is mostly as to the effect on the separation sequence. Therefore the development of a dynamic model version is focused on the distillation column and the integrated condenser reboiler unit, to be able to accurately capture external effects on product quality.

4.2.1 Distillation column model

The dynamic column model is in many ways similar to the steady-state one. Aside from a differnt formulation of the balances, hydraulic equations are needed. The necessary extension of the previous model are discussed in this section. The aim is to retain the capability for structural optimization for the dynamic models.

First the balance equations have to be rewritten in dynamic form. To do so reservoir terms or holdups are introduced. Namely the component holdups n_{ij} and internal energy U_j for each stage. With that

the component balance equations as presented in the previous section can now be rewritten as

$$\left(1-\sum_{k=1}^{j-1}\zeta_k^R\right)\frac{\mathrm{d}n_{ij}}{\mathrm{d}t} = \left(1+s_j^V\right)\cdot V_j\cdot y_{i,j} + \left(1+s_j^L\right)\cdot L_j\cdot x_{i,j} - V_{j+1}\cdot y_{i,j+1} - L_{j-1}\cdot x_{i,j-1} - \sum_{l=1}^{n_F}\zeta_{lj}\cdot F_j\cdot z_{i,j} - \zeta_j^R\cdot V_N\cdot y_{iN}, \quad i=1\ldots n_C-1,\quad j=1\ldots N,\quad k=1\ldots n_F,\quad l=1\ldots n_F. \tag{4.37}$$

While the internal energy balances become

$$\left(1-\sum_{k=1}^{j-1}\zeta_k^R\right)\frac{\mathrm{d}U_j}{\mathrm{d}t} = \left(1+s_j^V\right)\cdot V_j\cdot h_j^V + \left(1+s_j^L\right)\cdot L_j\cdot h_j^L - V_{j+1}\cdot h_{j+1}^V - L_{j-1}\cdot h_{j-1}^L - \sum_{k=1}^{n_F}\zeta_{kj}\cdot F_k\cdot h_j^F - \zeta_j^R\cdot V_N\cdot h_N^V, \quad i=1\ldots n_C,\quad j=1\ldots n_S,\quad k=1\ldots n_F. \tag{4.38}$$

The summation terms in front of the derivatives are needed if integer optimization is to be carried out with the model. In the steady-state case, no equilibrium took place at inactive stages. However in this case, there are the holdups in connection with the column hydraulics to be considered. While still no equilibrium should take place, even inactive trays will have to have a holdup. By means of the summations, the material balance is effectively transformed into a steady state equation, such that inactive trays will operate at steady-state with constant holdups, and therefore have no effect on the active part of the column.

In addition to the balance equations further constituent equations need to be introduced. From the steady state model we know the equilibrium equations

$$y_{ij} = K_{ij}\cdot x_{ij}, \qquad i=1\ldots n_C \quad j=1\ldots n_S, \tag{4.39}$$

and the summation equations

$$1 = \sum_i^{n_c} y_{ij} \qquad j=1\ldots n_S, \tag{4.40}$$

$$1 = \sum_i^{n_c} x_{ij} \qquad j=1\ldots n_S. \tag{4.41}$$

Furthermore defining equations for the accumulation of moles on each stage in vapour n_j^V and liquid n_j^L phase are needed

$$n_{ij} = x_{ij}n_j^L + y_{ij}n_j^V \qquad i=1\ldots n_C \quad j=1\ldots n_S. \tag{4.42}$$

These holdups will fill the volume of a given stage V_{stage}. Thus a volume constraint can be written as

$$V_{stage} = \frac{n_j^V}{\varrho_j^V} + \frac{n_j^L}{\varrho_j^L} \qquad j=1\ldots n_S. \tag{4.43}$$

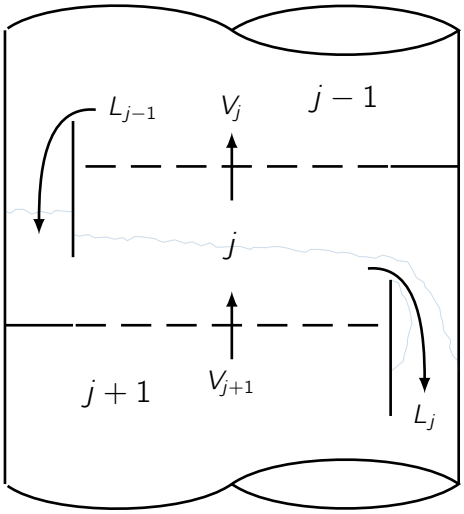

Figure 4.6: Column tray.

The internal energy in a stage corresponds to its enthalpy, reduced by pressure term

$$U_j = n_j^L \cdot h_j^L + n_j^V \cdot h_j^V - p_j \cdot V_{stage} \tag{4.44}$$

As we are no longer dealing in steady state hydraulic equations need to be introduced, which determine the liquid and vapour flow rates leaving a separation stage. As the mechanisms driving these flows might be very different depending on the type of internals used, it is not surprising that the corresponding equations are also very different. In the presented model implementation, both trayed columns and structured packings can be handled accordingly.

Trayed hydraulics

Trayed column hydraulics can be approximated by the following system of equations. All equations presented here were taken from [26].

The liquid flow rates are calculated from the well established francis formula , derived from the law of Bernoulli and taking effects like bubbling into account

$$L_j = \frac{2}{3}\sqrt{2g}\varrho_j^L \ell_{weir} \Phi h_{ow}^{\frac{2}{3}} \qquad j = 1 \ldots n_S. \tag{4.45}$$

Where h_{ow} denotes the height of the liquid over the weir, which can be calculated from the froth height h_f and the weir height h_w

$$h_{ow} = h_f - h_w. \tag{4.46}$$

While the weir height is a tray design parameter the froth height is computed from the clear liquid height and the relative froth density

$$h_f = \frac{n^L \, MW^L}{A_{active} \, \varrho^L \, \Phi}. \tag{4.47}$$

Lastly in terms of liquid flow rates, the relative froth density is dependent on the degree of aeration within the liquid, expressed by the aeration factor β from an empirical equation

$$\beta_j = 1 - 0.3593 \left(\frac{V_{j-1}\, MW^V_{j-1}}{A_{active}\sqrt{\varrho_{j-1}}} \right)^{0.177709} \qquad j = 1 \ldots n_S, \tag{4.48}$$

$$\Phi_j = 2\beta_j - 1. \tag{4.49}$$

The pressure difference between stages is the driving force for the vapour streams. The pressure drop is modeled as having two contributions, the dry and wet pressure drop. While dry pressure drop stems from the vapour flowing through the holes with in tray, the wet pressure drop is caused by the liquid holdup on the stage.

$$p_j - p_{j+1} = h^{liq}_j \varrho^L_j g + 0.5 \xi \varrho^V_{j+1} \left(\frac{q^V_{j+1}}{A_h} \right)^2 \tag{4.50}$$

Structured packing hydraulics

Structured packings and their hydraulic behaviour are currently still under investigation. The number of available correlations for calculation of internal flow-rates is much more limited than for trays or even dumped packings. Among the most established models is the one developed by Bravo et al. [38] at the University of Texas. This model has been extended to be valid in the loading region and account for different types of packing material [16]. As main linking factor between vapour and liquid flow-rates as well as the pressure drop, the liquid holdup has bee identified by the authors. It is expressed in dimensionless form h_t in terms of the corrugation side S, and the film thickness δ

$$h_L = \frac{4}{S}\delta. \tag{4.51}$$

One very important factor while estimating the hydraulic behaviour is the dry pressure drop per meter packing δp_{dry}. Within in the presented model it is estimated by

$$\delta p_{dry} = \left(\frac{\varrho^G}{\varrho_{air,1bar}} \right)^{0.4} \left(\frac{C_1 \varrho^G v_G^2}{S\epsilon^2 (\sin\Theta)^2} + \frac{C_2 \mu_G v_G}{S^2 \epsilon \sin\Theta} \right) \tag{4.52}$$

Another perquisite for calculating the holdup is the knowledge of the amount of wetted area of the available surface area within the packing. It seems reasonable to assume that this will be dependent on the characteristic of the liquid flow through the packing. To characterize the current, well known dimensionless numbers are used. Namely *Weber* (We), *Froude* (Fr) and Reynolds (Re) numbers

$$We = \frac{v_L^2 \varrho_L S}{\sigma}, \tag{4.53}$$

$$Fr = \frac{v_L^2}{Sg}, \tag{4.54}$$

$$Re = \frac{v_L S \varrho_L}{\mu_L} \tag{4.55}$$

With that an approximation for the holdup correction factor F_t due to partial wetting can be expressed as

$$F_t = \frac{A_1 \left(We\, Fr\right)^{0.15} S^{A_2}}{Re^{0.2}\, \epsilon^{0.6} (1 - 0.93 \cos\gamma)(\sin\Theta)^{0.3}} \tag{4.56}$$

$$h_L = \left(\frac{4F_t}{S}\right)^{\frac{2}{3}} \left\{ \frac{3\mu_L v_L}{\varrho_L \epsilon \sin\Theta g \left[\left(\frac{\varrho_L - \varrho_G}{\varrho_L}\right)\left(1 - \frac{\delta p}{\delta p_{flood}}\right)\right]} \right\}^{\frac{1}{3}} \tag{4.57}$$

4.2.2 Integrated condenser & reboiler unit

As it has been stated on several occasions the condenser reboiler unit is essential in the cryogenic air separation process. Even more so, when we consider the dynamics behaviour of the process. In order to model this unit, it is assumed that all vapour entering the stage will be condensed, thus the unit is regarded as total condenser. Furthermore the holdups on the condenser side are assumed to negligible. The reboiler side on the other hand is modeled as an equilibrium stage much like the stages within the column.

Reboiler side

As the reboiler side behaves like an equilibrium stage, the governing equations are very similar to those for a stage inside the columns. Hence they will be given without much further comment.

The material balances

$$\frac{\mathrm{d}n_i^{reb}}{\mathrm{d}t} = L_{reb}^{in} \cdot x_{i,reb}^{in} - V_{reb}^{out} \cdot y_i^{reb} - L_{reb}^{out} \cdot x_i^{reb}, \qquad i = 1 \ldots n_C. \tag{4.58}$$

Internal energy balance

$$\frac{\mathrm{d}U_{reb}}{\mathrm{d}t} = L_{reb}^{in} \cdot h_{in}^{reb} - V_{reb}^{out} \cdot h_V^{reb} - L_{reb}^{out} \cdot h_L^{reb} + Q_{CR}. \tag{4.59}$$

In addition to the balances the equilibrium and summation equations are necessary to complete the equations system.

As for the trays hydraulic equations determine the flowrates leaving the unit. For the liquid outlet Bernoulli's principle was used to derive an equation

$$L_{reb}^{out} = A_{\text{valve}} \varrho_L \sqrt{\frac{2 \cdot (\Delta p + \tilde{\varrho}_L g h)}{\tilde{\varrho}_L}}, \tag{4.60}$$

disregarding the height difference an equation for the vapour flowrate can be derived

$$V_{reb}^{out} = A_{\text{valve}} \varrho_V \sqrt{\frac{2\Delta p}{\tilde{\varrho}_V}}. \tag{4.61}$$

Condenser side

For a total condenser disregarding reservoir terms the mass balances become trivial

$$L_{con}^{out} = V_{con}^{in}. \tag{4.62}$$

To ensure bubble point temperature a summation as well as an equilibrium expression are included

$$1 = \sum_{i}^{n_C} K_i x_{i,con}, \qquad i = 1 \dots n_C, \tag{4.63}$$

$$x_{i,con} = y_{i,con}^{in}, \qquad i = 1 \dots n_C - 1. \tag{4.64}$$

An energy balance around the condenser side determines the transferred energy

$$Q_{CR} = L_{con} \cdot \left(h_{con}^{in} - h_{con}^{out}\right). \tag{4.65}$$

Heat exchange

As the transferred energy is determined form the condenser energy balance, the temperature difference between condenser and reboiler can be calculated by means of

$$Q_{CR} = \alpha A_{HX} \cdot \left(T_{con} - T_{reb}\right). \tag{4.66}$$

Roffel et al [39] found form process data, that the overall heat transfer coefficient (αA) can be approximated by a simple formula in terms of the condenser inlet vapour flowrate

$$\alpha A = c_1 \left(V_{con}^{in}\right)^{0.8}. \tag{4.67}$$

4.3 Thermodynamic models

Aside from the unit operation models, the behaviour of materials in a process needs to be adequately accounted for. This is done by means of so called equations of state (EOS) and excess Gibbs energy models. In terms of thermodynamics there are only a limited amount of variables. Namely the pressure, density and temperature as well as composition. While equations of state can model a given system in the vapour as well as liquid phase, excess Gibbs energy models only account for the behaviour of a liquid and need to be used in conjunction with other models for the vapour phase. However they have shown considerable better performance for highly non-ideal systems [2]. As mentioned earlier (sec. 4.1.3) it is essential to accurately capture the non-idealities of air in order to capture the liquefaction process. In the case of cryogenic air separation, the Peng-Robinson as well as the Benders equation of state have shown satisfactory performance. The Peng-Robinson

equation was chosen to be used in the presented model

$$p = \frac{RT}{V-b} - \frac{a_c\left[1+m\left(1-\sqrt{T_r}\right)\right]^2}{V^2+2bV-b^2} \tag{4.68}$$

$$m = 0.37464 + 1.54226\omega - 0.26992\omega^2 \tag{4.69}$$

$$a_c = 0.45724\frac{R^2T_c^2}{p_c} \tag{4.70}$$

$$b = 0.077796\frac{RT_c}{p_c} \tag{4.71}$$

$$\omega = -1 - \log_{10}\left(p_r^{sat}\right)_{T_r=0.7} \tag{4.72}$$

However the Peng-Robinson EOS relies on the so called one-fluid theory which models each fluid as pure. To model mixtures the pure component parameters have to be "mixed"

$$a = \sum_{i=1}^{C}\sum_{j=1}^{C} y_i y_j a_{ij}, \tag{4.73}$$

$$a_{ij} = \sqrt{a_i a_j}(1-k_{ij}), \tag{4.74}$$

$$b = \sum_{i=1}^{C} y_i b_i. \tag{4.75}$$

From that EOS numerous relevant properties such as excess enthalpy, fugacity coefficients or densities can be calculated. For a list of some relevant equations refer to sec. C.1.

4.4 Model implementation

As mentioned the presented models have been implemented in the process simulator gPROMS®. Although application to the cryogenic air separation process served as case where the model would be applied, the aim was to develop – especially in the case of the column models – a flexible model which could be used for a multitude of problems while trying to achieve a reasonable amount of complexity, such that a user mainly used to a pure flowsheeting environment should be able to apply the models with relative ease.

In the following sections first some general aspects of modeling in gPROMS® will be pointed out and the structure of the implemented model discussed in more detail. Subsequently several strategies for initializing the column model based on the previously model structure will be presented.

4.4.1 Model structure

When discussing the structure of gPROMS® models first some aspects of the modeling language have to be discussed. In this context CASE selectors, IF statements and the implementation

INITIALIZATION_PROCEDURE's in gPROMS® are most important. Within this section we will first briefly discuss those features and how they are used in gPROMS®. Afterwards it will be shown, how these structures are used, to create a model which can quickly be tailored the specific needs of a given user, and how distillation columns can be initialized within that framework.

IF statements and case selectors have many similarities as they can distinguish between different cases within a given model. For many applications they might even be used equivalently. As in almost all contexts the IF statements evaluates a condition and depending on wether it is fulfilled or not and evaluates differen formulae accordingly. A CASE statement distinguishes different branches between the model can switch during simulation or initialization. One major difference ist, that the number of equations in each CASE branch must match while for IF statements that condition is not enforced. However care must be taken when using these structures – especially during simulation – as they will in many cases introduce discontinuities. Furthermore when using IF statements one must distinguish, wether the evaluated statement is a parameter, or a variable in the model. Given it is a parameter, the statement will remain true (or false) for each instance of simulation. This introduces some flexibility in terms of diverging in the number of equations within model variants.

INITIALIZATION_PROCEDURE's are used – as the name suggests – to initialize models. The basic idea is to automatically solve a sequence of increasingly complex models, using the solution of a previous model as starting point for converging the current one. Furthermore the switch between models can be done within a either a so called JUMP_TO or MOVE_TO statement. Within the former there is a hard cut between the model variants, while in the latter a homotopic approach is employed to get form one model branch to another. While this should be the more robust solution, if the path of the homotopy remains in a feasible region, it necessitates greater care in terms of model robustness and scaling, as the internal integrator is used to move along the homotopic path.

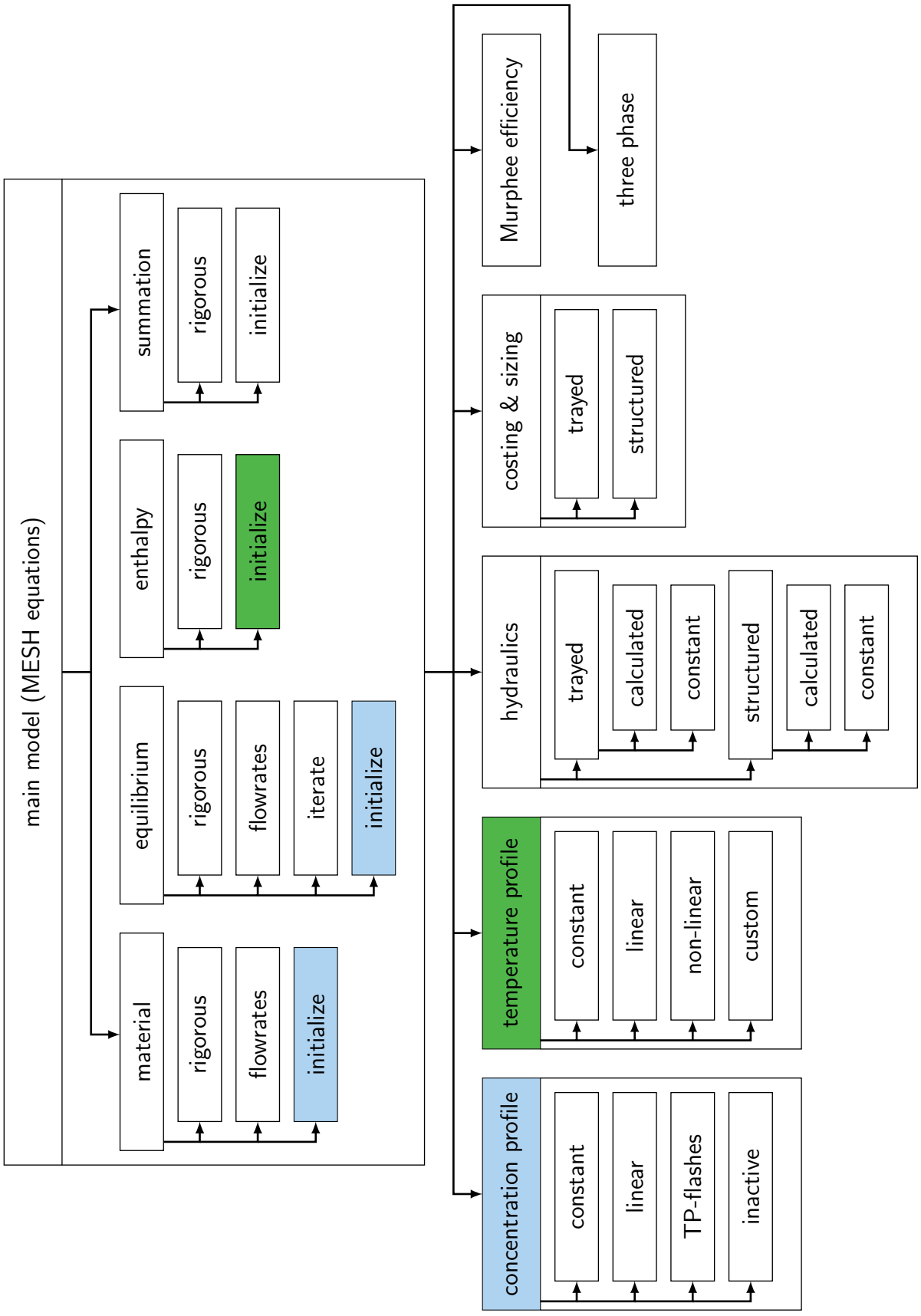

Figure 4.7: Distillation column model structure including sub-models and CASE branches.

The structure of the developed model is depicted in fig. 4.7. The main block denote separate model units that can, with the exception of the main model be activated or deactivated. The connections inside the main blocks denote selectors along with their possible branches.

The selective deactivation of sub-models is done by creating sub flowsheets and then assigning array of a respective model rather than a specific entity. By assigning an array size of zero, the model is effectively deactivated. This is done to reduce the number of variables and computational effort, if certain model capabilities are superfluous. for the rest of this section various model branches will be briefly elaborated upon. Within the main model, all branches labeled "rigorous" correspond to the equations as presented in sec. 4.1.1 and sec. 4.2. For the "flowrates" branches the mass balance has been written in terms of component flowrates rather than total flowrates and mole fractions. The "initilaize" branches of the material, equilibrium and energy selectors rely on the concentration profile and temperature profile sub-models to generate values, which are assigned straight forward to the respective variables. The reason those guesses were not directly implemented in the main model was to retain a level of flexibility of implementing alternative approaches without altering the general model structure. The meaning of the "iterate" branch within the equilibrium selector will be discussed in further detail in the next section.

The profile sub-models give several choices for initial profiles. In the case of the concentration profiles, the edge points will always be determined by a TP or vapour fraction flash of the mixed feed. While for temperature profile model the edge points can be either bubble and dew point temperature of the mixed-feed, or the feed temperatures of the highest (in terms of feed location) and lowest feed.

Having variable pressure along the column, sometimes greatly complicates initial convergence. Therefore can all hydraulics models be turned inactive, in which case they will return a constant previously assigned pressure drop for each stage.

The sub-model "three-phase" somewhat emulates calculations for the case when to liquid phases are present, as it needs to be ensured, that no wrongful information about the phase equilibrium is attained b y the model, which can for instance cause severe errors in the mass balance, while the overall model might still converge. It is simply assumed, that the liquid phases, while separate, are distributed in such a way, that the liquid phase might still be treated as a single phase. Hence in that case, the concentrations and enthalpies of both phases are mixed, while information about both phases is stored in appropriate variables.

4.4.2 Initialization procedures

This section deals with different initialization strategies for the distillation columns. Before going deeper into that topic, it needs to be pointed out, that physical property estimation in gPROMS® is done by means of so called foreign objects. Those are external objects, to which function calls along with the corresponding parameters can be passed and a return value or vector is returned. These calls range from simple properties like molecular weight of components to flash calculations in many variations.

As an initial remark it should be noted, that for all initialization procedures, if the hydraulic sub-model is activated, first an initial profile is assumed, and after the model has converged, the selector

within the hydraulics sub-model is switched to the calculated pressure drops. No problems with the hydraulics models were encountered, if the specified column geometry allowed for feasible column operations.

Initial specifications

One issue that comes up when giving specifications for a column is, that not all specifications are compatible with the the used initialization procedure. Specifically this is the case for specified duties purities or temperatures as they cannot be considered in the initialize branches.

For those cases it is necessary to supply alternative specifications, namely a reflux or boil-up ratio or any flowrate, which can be fulfilled during initial calculations. Additionally, if "extreme" specifications are given such as very high purities, or extremely low flowrates, convergence might with a given procedure might fail. One strategy, that has proven fruitful in those cases, was to supply a more moderate specification, initialize and converge the model up to the rigorous branches and then switch to the more complex specification. Especially when the switch is made in the rigorous branch, chances are hight, that the solution, if a MOVE_TO switch is employed, will only pass through feasible regions and a final solution can be attained.

These initial specification can be used in conjunction with all initialization procedures discussed in the following sections.

Flash initialization

The flash initialization, is the simplest, but nevertheless a very effective and efficient way of initializing the model. As initial guess constant profiles are assigned for vapour and liquid concentrations taken from the aforementioned feed flash. For the temperatures a linear profile between dew and bubble point temperature of the feed flash is used. The vapour and liquid flowrates are computed from the constant molar overflow assumption while considering sub-cooled or super-heated feed streams. In terms of the model this strategy translates into starting all selectors in the initialize branches and then simultaneously switching all selectors to the rigorous branches.

Linearized material balance

As discussed in the example given in sec. 4.1.1 this initialization procedure relies on on first initializing the model as for the flash initialization. Afterwards, in an intermediate step, the enthalpy and summation branch are kept in the initialize branch, which means, the initial temperature profile is kept fixed, and the constant molar overflow assumption retained. The material and equilibrium selectors are then switched to the flowrates branches, where a linearized material balance is solved with constant equilibrium ratios and molar flowrates. The constant equilibrium ratios are enforces, by passing the values from the concentration profile sub-model to the physical property calls, rather that the actual computed values for molar concentrations.

The main reason for formulating this mass balance in terms of component flowrates is, that due to the assumptions a solution will yield discrepant results. Especially if the equilibrium ratios in the

converged solution span a large range of values. Due to these discrepancies some molar fractions might even become negative. As the corresponding variable type is bounded to zero or a small negative number, this might cause the solver to fail during convergence of this step.

Furthermore the molar fractions would also have to be re-normalized, as the summation to one is not enforced in this case.

Afterwards all selectors are again switched to the rigorous branch.

```
INITIALISATION_PROCEDURE
  START
    material    := initialize ;
    equilibrium := initialize ;
    energy      := initialize ;
    summation   := initialize ;
    side_scale  := 0 ;
    hydraulics  := constant ;
  END
  NEXT
    JUMP_TO
      material    := flowrates ;
      equilibrium := flowrates ;
    END
  END
  NEXT
    JUMP_TO
      REVERT material ;
      REVERT equilibrium ;
      REVERT energy ;
      REVERT summation ;
    END
  END
  NEXT
    MOVE_TO
      side_scale := 1 ;
    END
  END
  NEXT
    JUMP_TO
      REVERT hydraulics ;
    END
  END
```

Iterative approach

Previously it has been said, that the inside-out algorithm has proven very robust when it comes to solving complex distillation problems. However it is based on an modular iterative approach which is incompatible with equation based process simulators.

One of the main aspects is to construct simplified models for enthalpies and the equilibrium, which only give accurate results for the point they have been constructed at, but are much better behaved, than rigourous enthalpy and equilibrium correlations. In eat step of the iteration a new model for the physical properties is constructed, at the point, where the previous model evaluation with the previous physical properties model converged to. The iterative process terminates, when no further (or very little) changes occur in the newly constructed parameters for the new physical property models.

In order to mimic such an approach in gPROMS®, the branch "iterate" within the equilibrium selector has been created. There the physical properties are called with an new set of concentration variables, which are assigned arbitrary values in all other branches. To do the iterations anther structure of gPROMS® is used. So called TASKS. With that it becomes possible, to converge a the model, with a given concentration stored in these variables, and after convergence, replace those values with the current values of liquid and vapour mole fractions.

The drawback however, is that the number of iterations to be carried out needs to be specified in advance. This strategy, while rather time consuming due to large overhead in computational time during execution of the TASK, has generated very promising results and with it it was possible to converge columns with very complex multi-component systems.

```
SEQUENCE
  i := 1 ;
  WHILE i < number_of_iterations DO
    SEQUENCE
      PARALLEL
        REASSIGN
          column_section.x_iterate(,) := OLD(column_section.x(,));
          column_section.y_iterate(,) := OLD(column_section.y(,));
        END
        SWITCH
          column_section.phase_equilibrium
            := column_section.iterate_to_rigorous;
        END
      END
      i := i + 1 ;
    END
  END
  SWITCH
    column_section.phase_equilibrium := column_section.rigorous;
  END
END
```

Side draws

During construction of process flowsheets and application of the developed models it turned out, that columns with side draws add extra complexity in terms of initialization. To accommodate that fact side draw versions of the previously described initialization procedures have been developed. The only difference is, that the side draws are initially set to zero once convergence has been achieved, they are again set to their specified values. Either by an instant change or again in a continuous fashion.

5 Process model application

The desired outcome of implementing process models is to be able to predict process behaviour such that a lot of experiments can be replaced by simulation runs. Beyond simulating a process, it is also possible to optimize process design and operation. In this section the previously discussed models are applied in various ways to gain insight into the aforementioned example process (sec. 2).

The following chapter is structured as follows. Initially some theoretical considerations as to how the examined class of problems, namely discrete-continuous, can be solved. This is followed by the description of several applications for the steady-state and dynamic models. As for the implementation, several things have to be considered, when applying these models. Some intricacies of model implementation and application are discussed in the last section.

5.1 MINLP solution techniques

In this section two different solution approaches for mixed-integer non-linear programs (MINLP) will be presented. The problem considered here in its most general form can be written as

$$\begin{aligned} \min_{x,y} \quad & C = f(x,y) \\ \text{s.t.} \quad & g_j(x,y) \leq 0, \;\; j \in \mathcal{J} \\ & x \in \mathcal{X}, \; y \in \mathcal{Y} \end{aligned} \tag{P1}$$

where $\mathcal{J}$ denotes the set of all constraints while $\mathcal{X}$ and $\mathcal{Y}$ denote the set of continuous and integer variables respectively.

The main focus lies on discussing two alternative solution approaches to the aforementioned class of problems. First the outer approximation algorithm, which is implemented in gPROMS®, is introduced. Then then an alternative approach to solve this class of problems, based on a continuous reformulation of the discrete decision variables, which has recently been proposed [24, 43] will also be discussed. Both approaches will later be applied to the example process and compared in terms of optimality, time consumption and robustness.

5.1.1 Outer approximaltion

The outer approximation (OA) algorithm relies on consecutively solving two sub-problems in order to converge to a solution. These problems are an NLP sub-problem, in which all integer values are fixed, as well as a linearized version of the original MINLP (P1).

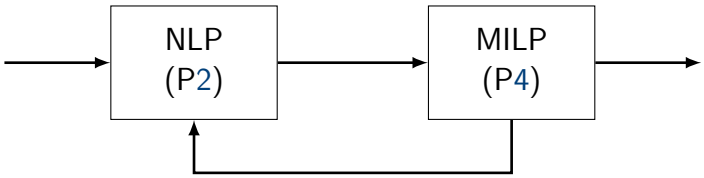

Figure 5.1: Outer approximation algorithm.

First we consider the continuous sub-problem. Keeping all integer values constant results in the following NLP

$$\begin{aligned} \min_{x} \quad & C_{LB}^{k} = f(x, y^k) \\ \text{s.t.} \quad & g_j(x, y^k) \leq 0, \quad j \in \mathcal{J} \\ & x \in \mathcal{X}. \end{aligned} \tag{P2}$$

where the index k denotes the values for the k^{th} iteration. If (P2) is infeasible the NLP feasibility subproblem for fixed y^k can be solved.

$$\begin{aligned} \min_{x} \quad & u \\ \text{s.t.} \quad & g_j(x, y^k) \leq u, \quad j \in \mathcal{J} \\ & x \in \mathcal{X}, \quad u \in \mathbb{R} \end{aligned} \tag{P3}$$

This NLP returns a strictly positive value for u.

Aside from the presented NLP's a linearized version of (P1) is regularly solved

$$\begin{aligned} \min_{x,y} \quad & C_{L}^{k} = \alpha \\ \text{s.t.} \quad & f(x^k, y^k) + \nabla f(x^k, y^k)^T \begin{bmatrix} x - x^k \\ y - y^k \end{bmatrix} \leq \alpha \\ & g_j(x^k, y^k) + \nabla g_j(x^k, y^k)^T \begin{bmatrix} x - x^k \\ y - y^k \end{bmatrix} \leq 0, \quad j \in \mathcal{J} \\ & x \in \mathcal{X}, \quad y \in \mathcal{Y}, \quad k = 1 \dots K \end{aligned} \tag{P4}$$

The linearized problem can be constructed in several ways from the set of points K attained in previous iterations. Sometimes only violated or active constraints are linearized. When objective function and constraints are convex, the objective function is underestimated, while the constraints are overestimated. From the overestimated constraints stems the name outer approximation.

Each solution of the NLP with fixed y^k yields a new point (x^k, y^k) which is used to construct an updated version of the MILP. The MILP generally includes linearized versions of all constraints and the objective function. As more and more points become available during the iterative process, new constraints are constructed for each available point.

The main theorem for the derivation of the OA algorithm states, that the optimal solution of the problem (P4) constructed from all points $(x^k, y^k), k \in K^*$. Where K^* is made up of all optimal

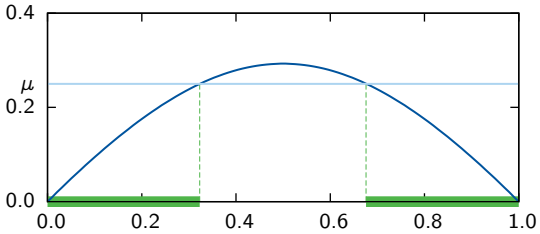

(a) plot of Fischer-Burmeister function.

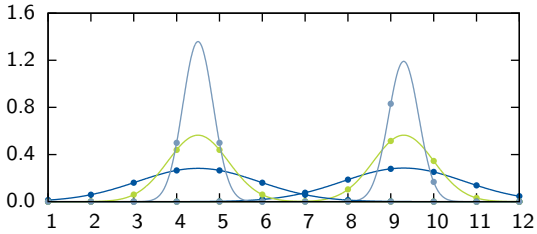

(b) plot of DDF function.

solutions of (P2) where the current y^k yields a feasible solution, and (P3) where infeasible solutions of the NLP with fixed y^k are encountered. It should again be emphasized, that this theorem holds only for convex a objective function and constraints.

As the points necessary to construct the aforementioned system are not available when the solution process commences, a smaller systems is constructed and extended as more points become available. Initially again the fully relaxed problem is solved. This again yields an absolute lower bound for the original problem. The solution of each consecutive MILP gives a new lower bound which will always be greater than the bounds from previous iterations. Without any prove this argument is supported by the fact that adding new linear constraints will limit the feasible region of the problem and hence further restrict the possible solutions for the continuous variables.

The optimal points attained from the NLP subproblems with fixed discrete values form upper bounds on the optimal solution. Here no statement can be made about the quality of the bound in each step, but rather is the current upper bound updated, once a lower value is encountered.

The iterative process terminates, once the current upper and lower bound are within a given tolerance. It can be pointed out, that the outer approximation algorithm converges to the optimal solution in a single iteration if objective function and constraints in the original problem are linear, since in that case problems (P1) and (P4) are equivalent.

5.1.2 Continuous reformulation

An alternative approach to solving discrete-continuous problems is to reformulate them as NLP and introduce further constraints which ensure that the discrete decision variables will assume integer values. Several different authors have proposed ways of reformulating integer decisions. One common way is to introduce the so called complementary or equilibrium constraints which lead to problems that must be dealt with designated (NLP) solvers. Despite the fact that they posses poor theoretical features they have successfully been applied to problems of different scales. Lately however, alternative approaches have been suggested, which can be implemented in gPROMS® with relative ease and then solved with the NLP solvers included in the modeling environment. The first approach presented formulates a so called non-linear complementary problem (NCP) by introducing further constraints. Secondly within the distributed stream method, differentiable distribution functions (DDF) are formulated to model the associated integer decisions. In the following both approaches will be summarized briefly. A more detailed discussion of continuous reformulation techniques can be found in [43].

Non-linear complementary problem (NCP)

To arrive at a formulation with favourable theoretical properties Kraemer et al. [23] proposed a continuous reformulation based on the Fischer-Burmeister function

$$1 - \sqrt{y_i^2 + (1 - y_i)^2} = 0. \tag{5.1}$$

The zero set of this function contains exactly the values zero and and hence forces a continuous variable to take either integer value. However it is still very hard to solve complex, large-scale problems by simply enforcing this constraint. In order to facilitate convergence, the FB-function can be relaxed to a fully continuous problem

$$1 - \sqrt{y_i^2 + (1 - y_i)^2} \leq \mu. \tag{5.2}$$

The relaxation factor μ is then gradually reduced to zero in a sequence of NLP problems. Fig. 5.2a shows a plot of the FB-function over the domain zero to one. The green lines on the x-axis denote the feasible domain for a given value of μ. As one can see, if the relaxation factor is chosen large enough the entire span between zero and one is feasible, while for decreasing values the feasible set becomes disjunct and continuous variables are forced to either side to take on integer values.

Differentiable distribution function (DDF)

An alternative way of reaching a continuous formulation was brought fourth by Lang and Biegler [25] who within their distributed stream method propose the introduction of a differentiable distribution function (DDF)

$$\Psi_j = \frac{\exp\left[-\left(\frac{j-\sum_i \zeta_i i}{\sigma}\right)^2\right]}{\sum_k \exp\left[-\left(\frac{k-\sum_i \zeta_i i}{\sigma}\right)^2\right]}. \tag{5.3}$$

This function models a normal distribution around a central tray. As the standard deviation (σ) is reduced, the spike at a given tray becomes more significant. Again in a series of NLP's σ is driven to small value. At $\sigma = 0.25$ one can numerically consider the solution as integer. Fig. 5.2b shows a plot of the DDF function for a continuous stage value of 4.5 and 9.3 at $\sigma = 2, 1, 0.5$. Please note, that the values for each stage, denoted by dots, must add up to one. Depending on the distribution, a continuous plot can take on values larger than one.

5.2 Steady-state models

There are several ways in which a process model in general, and the steady-state models in particular can be used. In this case, all models have been implemented with the use for operational and structural optimization in mind.

This section begins, with a discussion of the degrees of freedom, coupled with feasible specifications. Linked to this matter is the crucial question of model initialization, which is dealt with in the subsequent section. Finally a look at different optimization setups concludes this section.

specification	replacement for H_1	replacement for H_N
reflux or boilup ratio	$0 = L_1 - \nu^D \cdot (V_1 + S_1^L)$	$0 = V_N - \nu^R \cdot L_N$
temperature	$0 = T_1 - T_{spec}$	$0 = T_N - T_{spec}$
product flowrate	$0 = (V_1 + S_1^L) - D$	$0 = L_N - B$
component product flowrate		$0 = L_N \cdot x_{iN} - b_i$
mole fraction	$0 = y_{i1} - y_{i,spec}$	$0 = x_{iN} - x_{ispec}$

Table 5.1: discrepancy functions for different column specifications.

5.2.1 Degrees of freedom

The equation systems presented above is comprised of $n_S n_C$ component balances and equilibrium equations, $2n_S$ summation equations and n_S energy balances. This gives a total of $n_S(2n_C + 3)$ equations. On the other hand there are n_S temperatures and pressures, $2n_S$ molar flow rates, n_S energy streams, and $n_S n_C$ vapour as well as and liquid concentrations. Additionally the feed flow rates compositions and temperatures and the side draw split fractions or flow rates appear as variables. The feeds and side draws would usually be specified, which leaves a total of $n_S(2n_C + 5)$ variables.

The pressure profile of a distillation column is usually specified. In terms of unit operations this pressure drop is of high significance, as many columns can only be feasibly operated if the pressure drop does not exceed certain limits. In case of the ASU the production of Argon only became feasible as structured packings, which display a very low pressure drop, became available. This is due to the large number of theoretical stages required to attain the desired Argon purities.

The energies Q_i denote addition heaters or cooler on the respective stages. For all intermediate stages these values would be specified as well. If all energies are specified, that would – along with the pressure profile – sum up to $2n_S$ specifications, which leaves $n_S(2n_C + 3)$ unknowns. As the number of equations and unknowns are the equal, this system is then well specified.

In practice it is often challenging to correctly guess the condenser and reboiler heat loads in advance. This is especially true since they have a tremendous impact on the overall performance of the column. Hence it is often desirable to supply other specifications than the respective heat loads. To allow for such specification so called discrepancy functions can be introduced [17], which replace the energy balance for the condenser and / or reboiler stage.

One common specification is the so called reflux ratio $\nu^D = \frac{L_1}{V_1 + S_1^L}$ for the condenser, or the boil-up ratio $\nu^R = \frac{L_N}{V_N}$ for the reboiler. They are defined as the ratio of the molar flowrate sent back into the column over the product flowrate which leaves the column. For the reboiler this denotes a liquid stream, while for the condenser the product can be gaseous and liquid. Specifying this leads to

$$0 = L_1 - \nu^D \cdot (V_1 + S_1^L), \tag{5.4}$$

$$0 = V_N - \nu^R \cdot L_N, \tag{5.5}$$

as discrepancy functions. In addition to that further specifications are conceivable. Most commonly distillate (D) or bottoms (B) flow rates, purities, component flow rates (d_i, b_i) or temperatures. The corresponding discrepancy functions are summarized in tab. 5.1.

The specifications for the reboiler stage are quite straightforward, in contrast to that, for the condenser different cases have to be considered. In the most general case the top product can be drawn as

vapour and liquid. This case is here called a partial vapour liquid condenser. The other cases are a total condenser, where all the vapour entering the condenser stage is condensed, and all product is drawn as a liquid stream, as well as a partial vapour condenser, where only the reflux is condensed and all product is drawn as vapour. As discussed earlier no VLE takes place in the condenser stage, if a total condenser is specified, which needs to be accounted for. Both the total and partial vapour condensed implicitly include an extra specification since in former case the top vapour product flow rate becomes zero and in the latter the top liquid product flowrate. Furthermore a specification of the condenser energy is infeasible as well as implicitly given for the total condenser. In case of the partial vapour liquid condenser no implicit specification is given, which requires an additional specification. In general two top specifications are necessary, whereas only one bottom specification is required. These top specification can include the condenser duty, any top flowrate, the reflux ratio as well as a newly introduced quantity, the top vapour fraction defined as

$$\nu^{vap} = \frac{V_1}{V_1 + S_1^L}. \tag{5.6}$$

5.2.2 Model initialization

As mentioned before the solution of the MESH equations can pose a considerable problem to numerical solvers. It is therefore necessary to supply the solver with feasible estimates for the involved variables that can be used as an initial guess for convergence of the process model. A lot of effort has been spend to formulate robust strategies to initialize distillation column models. One of the most prominent is the so called Inside-Out algorithm first introduced by Boston and Sullivan [6]. Within this algorithm an inner and outer iterative loop are employed. Within the outer loop approximate parameters for simplified models of phase equilibrium and enthalpy are computed by rigorous thermodynamic models and guesses for stage temperatures and concentrations. Within the inner loop new stage temperatures and concentrations are attained by solving the MESH equations using the simplified thermodynamic models. Once the inner loop converges the simplified model parameters are updated within the outer loop by means of the newly calculated temperatures and concentrations. This algorithm converges in many cases even for very poor initial guesses and has been extended to handle complex columns with side-draws and even reactive distillation [5]. It is still in use in the process simulator Aspen Plus®. However as it is used within an modular algorithmic environment it is not applicable to equation based simulators such as gPROMS®.

More recently other approaches have been published to attain improved initial guesses. Fletcher and Morton [14] proposed the solution of a column model at infinite reflux and zero feed flow rate. This leads to a much simplified model which can be solved more easily. The computed purities and stage numbers can give valuable insight into the process model. As this approach relies on the solution of a simplified model and has no algorithmic elements, it can be implemented in equation based process simulators.

Another strategy that has been successfully applied to zeotropic and azeotropic mixtures relies on solving the column model for the limiting case of the adiabatic column [4]. The adiabatic column in this case is the column with the minimal entropy production in a real column. To avoid entropy

production all streams that come in contact must be in equilibrium. To achieve this the column would have to employ an infinite number of stages and have an infinite number of heat exchangers along its length. The adiabatic column then uses only two heat exchanger in the condenser and reboiler stage and assumes a pinch point at the feed stage.

A much simpler approach has proven adequate for many applications [17]. This approach is also employed as a starting point in this work. Therein feed properties are used as initial guesses. First a linear temperature profile form the boiling temperature to dew temperature of the combined feed mixture is used to initialize temperatures, whereas a simple flash at average column pressure and feed temperature yields a vapour and liquid concentration which is used as uniform profile for every column stage. However as the feed might be sub-cooled liquid or super-heated vapour, the TP-Flash is replaced by a specified vapour fraction. As vapour fraction for the flash initial estimates of the vapour and liquid flow rates at the top and bottom of the column are used. The stage-wise molar flow-rates are computed from the constant molal overflow assumption, which postulates a constant heat of vaporization and yields therefore uniform liquid and vapour flow-rates within a column section. A section in this case is denoted by any feed location where the flow-rates change due to the added feed. In the feed stages a super heated or sub-cooled feed is also considered by means of an extended vapour fraction

$$q^F = \frac{h^F - h^L}{h^V - h^L}. \tag{5.7}$$

While this approach leads to model convergence in many cases, it is not entirely robust. While the system considered in this case displays only moderate non-idealities it is highly cupeled. Especially the low pressure column (LPC) has multiple feeds and side draws, which leads to non-convergence if the aforementioned initialization strategy is employed. However the fact that the system is not highly non-ideal can be exploited. Whenever the K-values are not too much dependent on mixture composition an intermediate step can be used to refine concentration guesses. The constant molal overflow assumption is retained and the equilibrium ratios are computed based on the initial guesses from the first stage. The component balance is then reformulated only in terms of liquid component flow-rates l_{ij}

$$\begin{aligned} 0 = \left((1 + s_j^V) \cdot K_{ij} \cdot \frac{V_j}{L_j} + (1 + s_j^L)\right) \cdot l_{ij} - \frac{V_{j+1}}{L_{j+1}} \cdot K_{ij+1} \cdot l_{ij+1} - l_{ij-1} \\ - F_j^V \cdot z_{i,j}^V - F_j^L \cdot z_{i,j}^L, \qquad i = 1 \dots n_C \quad j = 1 \dots n_S. \end{aligned} \tag{5.8}$$

eq. (5.8) is linear in the liquid component flow rates. Furthermore vapour component flow rates are substituted in the linear component balance and can be computed by

$$v_{ij} = K_{ij} \cdot \frac{V_j}{L_j} \cdot l_{ij} \qquad i = 1 \dots n_C \quad j = 1 \dots n_S. \tag{5.9}$$

On of the reasons eq. (5.8) is formulated in terms of component flow rates rather than molar fractions, is that the molar fraction computed in that manner would not be normalized. If the mole fractions are computed from the component flow rates normalization is implicitly given

$$x_{ij} = \frac{l_{ij}}{\sum_k^C l_{kj}} \qquad i = 1 \dots n_C \quad j = 1 \dots n_S, \tag{5.10}$$

$$y_{ij} = \frac{v_{ij}}{\sum_k^C v_{kj}} \qquad i = 1 \dots n_C \quad j = 1 \dots n_S. \tag{5.11}$$

The total molar flow rates used in eq. (5.8) are computed by solving stage-wise total mass balances under the constant molal overflow assumption. This assumption postulates that the heat of vaporization is independent of system composition. Therefore always the same amount of liquid enters and leaves a given stage

$$0 = L_j + S_j^L - L_{j-1} - (1 - q^F) \cdot F_j \qquad j = 1 \dots n_S. \tag{5.12}$$

The vapour total flow rates are then computed from the total mass balances

$$0 = L_j + S_j^L + V_j + S_j^V - L_{j-1} - V_{j+1} - F_j \qquad j = 1 \dots n_S. \tag{5.13}$$

As no energy balances are included at this stage, the condenser and reboiler stage are characterized by the reflux ($\nu^c = \frac{V_1}{L_1}$) or boilup ratio ($\nu^r = \frac{V_N}{L_N}$) respectively. This leads to

$$0 = V_1 - \nu^c \cdot L_1, \tag{5.14}$$
$$0 = L_N - \nu^r \cdot V_N. \tag{5.15}$$

To close the equation system the global mass balance is included

$$0 = V_1 + L_N + \sum_{j=1}^{N} (S_j^V + S_j^L - F_j), \qquad j = 1 \dots n_S. \tag{5.16}$$

For more complex systems more elaborate strategies have been developed, which essentially try to incorporate some of the principals from the inside out algorithm into an equation based environment. The process simulator gPROMS® allows for definition of standardized initialization procedures as well as different model variants that can be solved consecutively. With that strategies were developed that proved successful for more complex mixtures and even three phase systems. As these strategies are closely linked to the implementation in gPROMS® and the programm capabilities, they will be discussed in sec. 4.4

Furthermore ist should be noted, that not all specifications are compatible with the initialization strategies described above. While this issue has been addressed, it also will be explained in the implementation section.

Example To illustrate how the initialization procedure works an example has been constructed of a rather complex column – or column section – with multiple feeds and side draws (fig. 5.2). It is taken from an example process of cryogenic air separation. The column in question is a column section without an condenser stage and displayed the most difficulties in terms of convergence when constructing the process flowsheet.

In addition to the aforemention initialization strategy, columns with side draws present are handled in a slightly different manner. Initially the side draws are disregarded. Then the initialization procedure is carried out. Once the column without side draws has converged, a homotopy approach

$$f(\mathbf{x}) = (1 - \alpha) \cdot f_0(\mathbf{x}) + \alpha \cdot f_1(\mathbf{x}) \tag{5.17}$$

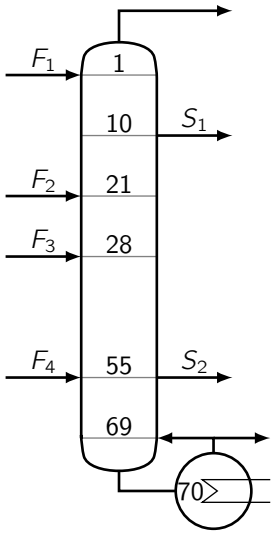

Figure 5.2: example column.

stream	flow $[\frac{kmol}{hr}]$	$z_{O_2}[-]$	$z_{N_2}[-]$	$z_{Ar}[-]$	$T[K]$	$p[bar]$
F_1	2985.77	4.674E-10	0.9999	6.378E-7	79.45	1.3
F_2	1836.36	0.2095	0.7812	0.0093	98.91	1.3
F_3	7609.06	0.2920	0.6950	0.0130	81.88	1.3
F_4	774.94	0.9161	5.393E-12	8.394E-2	92.13	1.8

stages	S_1 frac	S_2 frac	boilup ratio	p^{top}	p^{bot}
70	10	0.15	3.5	1.2 bar	1.3 bar

Table 5.2: column specifications.

is employed, where the parameter α is initially set to zero and then gradually moved to a value of one. During the initialization homotopies could generally be employed to move from one step to another. While in some cases robustness is improved by such a strategy, it is always computationally far more expensive then simply jumping between different stages.

For clarity reasons the different steps of the initializations procedure a repeated in a tabular manner

1.
   - linear temperature profile between dew (T^{dew}) and bubble point temperature (T^{bub}) of mixed feed.
   - linear profile between feed flash vapour and liquid compositions for liquid stage compositions.
   - constant profile for vapour compositions.
   - molar flow rates from constant molar overflow model.
   - side draw flow rates set to zero.
2.
   - total molar flow rates form constant molar overflow model.
   - simplified equilibrium ratios from initial liquid mole fractions and linear temperature profile.
   - liquid and vapour mole fractions from linearized mass balances.
3. rigorous solution of MESH equations with side draws still set to zero.
4. homotopic approach to MESH equations with side draws considered.

The resulting profiles for oxygen and nitrogen concentrations in the example column can be seen in fig. 5.3a and fig. 5.3b.

5.2.3 Steady-state optimization

Initially optimizations were carried out using the steady-state process models. While an effort has been made to create a realistic scenario, the main focus of this section is to demonstrate optimization

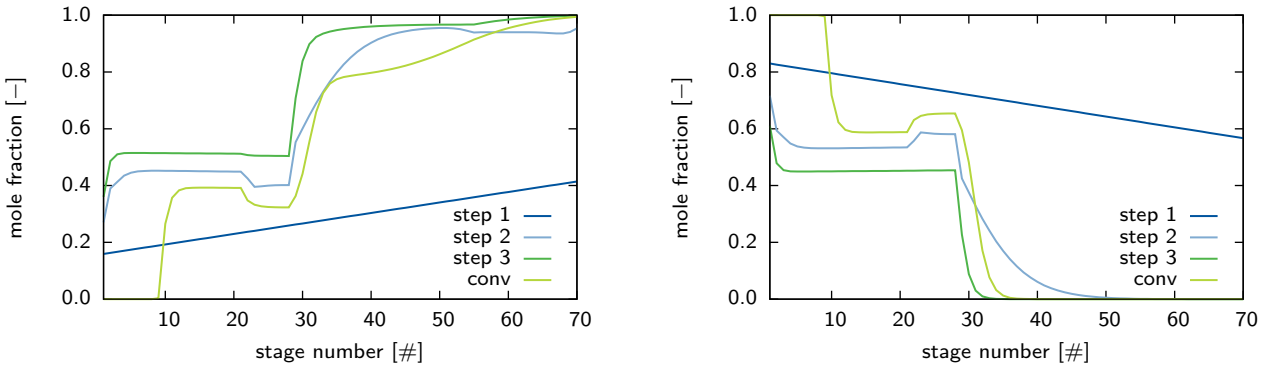

(a) oxygen concentration profiles.

(b) nitrogen concentration profiles.

Figure 5.3: initialization example concentration profiles.

	steady state 1			steady state 2		
variable name	result OA	result FB	deviation	result OA	result FB	deviation
objective function	**334702**	**328219**	**1.94 %**	**346320**	**346142**	**0.05 %**
plant air flowrate	12434.6	11703.0	5.88 %	12068.3	11981.1	0.72 %
CAC column diameter	1.23543	1.16392	5.79 %	1.10699	1.12137	1.30 %
CR CAC reflux ratio	37.7408	33.6728	10.78 %	39.6848	41.5425	4.68 %
CR main reflux ratio	4.12825	3.80242	7.89 %	2.54161	2.33128	8.28 %
HPC column diameter	2.90256	2.80806	3.26 %	2.88641	2.85296	1.16 %
HPC GN2 draw flowrate	1945.52	1870.20	3.87 %	532.432	839.935	57.75 %
LPC column diameter	3.93352	3.79809	3.44 %	4.13233	4.06009	1.75 %
waste draw flowrate	7414.57	7082.99	4.47 %	7088.12	7331.58	3.43 %
CAC draw flowrate	738.246	662.048	10.32 %	581.302	608.020	4.60 %

Table 5.3: steady-state optimization results - continuous variables.

capabilities within the model environment gPROMS® and to compare different solution approaches for complex discrete-continuous problems.

Single steady-state operation

In a first case operations for two separate steady-states were optimized. However only structural decisions on the columns were made along with the columns operational parameters. The solutions from both algorithms are summarized in tab. 5.3 and tab. 5.4, where the for contains the results for all continuous decisions and the latter all discrete decisions. Results attained by outer approximation are labelled as "OA" and by solving the NCP as "FB".

	CAC N	HPC N	LPC N	LPC F1	LPC F2	LPC F3	LPC S1	LPC S2
steady-state 1 OA	45	12	45	13	9	26	7	26
steady-state 1 FB	44	13	47	10	7	23	6	23
steady-state 2 OA	47	10	45	8	8	22	8	22
steady-state 2 FB	45	12	46	8	6	21	6	21

Table 5.4: steady-state optimization results - discrete variables.

	steady state 1		steady state 2	
	results OA	results FB	results OA	results FB
total time [s]	4847.88	1184.52	2971.09	843.39
CPU time [s]	26.72	225.72	43.94	201.99
MINLP	84	0	68	0
NLP	822	85	687	68
line search steps	2069	114	1088	87

Table 5.5: steady-state optimization results - time consumption.

	steady state 1		steady state 2	
variable	lower bound	upper bound	lower bound	upper bound
nitrogen product flowrate	3300	10000	3000	10000
nitrogen product purity	0.999	1.0	0.995	1.0
oxygen product flowrate	1700	10000	1600	10000
oxygen product purity	0.995	1.0	0.999	1.0
argon product flowrate	20	10000	15	10000
argon product purity	0.995	1.0	0.995	1.0
CAC diameter constraint	0	10	0	10
LPC diameter constraint	0	10	0	10
HPC diameter constraint	0	10	0	10

Table 5.6: steady-state optimization constraints.

The objective function considers only capital cost for the separation sequence

$$CAPEX = \left(\sum_{c} C_c^{\text{cap}} \right) \cdot \left(q^{-a} \frac{q^a - 1}{q - 1} \right), \qquad c = \{\text{HPC}, \text{LPC}, \text{CAC}\}. \tag{5.18}$$

The difference between the steady-states lies in the requirements on product flow rates and purity. Hence the different constraints enforced for the respective operation modes are summarized in tab. 5.6.

When solving the continuous reformulation of the problem, an extra constraint for each integer variable in form of the relaxed Fischer-Burmeister function was added. Furthermore the closure condition for each location decision was added as an equality constraint. This closure condition needs not to be explicitly considered using the outer approximation approach, since this is handled internally by declaring so called special ordered sets of type one. This allows gPROMS® and the outer approximation algorithm to exploit the special structure of the problem due to the *exclusive or* decisions.

In order to compare the results of the different solution approaches, various aspects can be taken into consideration. Foremost the objective value is a measure of performance. As the complexity of the underlying problem increases, the matter of time becomes a – sometimes limiting – factor. Therefore the time in which a solution is found, is a measure for the algorithm performance as well. However before the results are discussed in greater detail, some further aspects are worth mentioning.

In the process of solving the continuously reformulated problem, some difficulties arose. While (almost) integer values were found for most structural decisions, even during the initial iteration, especially the LPC column displayed some convergence problems. As the relaxation factor is reduced, the the feasible region between zero and one is is divided into two disjunct regions which become

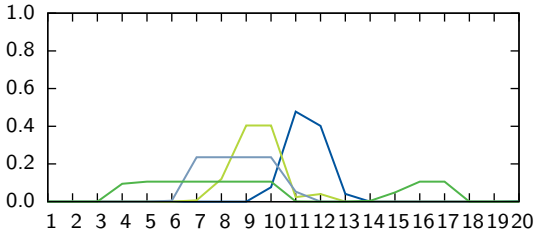

Figure 5.4: NCP convergence failure.

smaller and smaller. In some cases the solutions remain on one side of the feasible domain, namely the one converging to zero, while still fulfilling the closure constraint. As the relaxation factor is reduced, the solver is no longer able to "make the jump" to the other side of the domain. This leads to a distribution of small values for the split variables along the column. Fig. 5.4 shows a typical example for this type of convergence behaviour. After the initial NLP the feed is somewhat evenly distributed between two stages, neither really dominant. As the relaxation is tightened, the values are reduced, and distributed among more stages to fulfil the closure condition. As the relaxation factor approaches zero the closure condition can no longer be satisfied, which leads to violation of the equality constraint and convergence failure.

This issue has been addressed, by [24] who propose a re-initialization strategy based on the magnitude of the Lagrange multipliers associated with the continuous variables. While the results using this adjusted strategy are very promising it could not be implemented within the scope of this thesis. In addition to the adjusted algorithm, the problem formulation can be altered to improve convergence of the solution algorithm. Two strategies can be employed, which exploit the structure of the distillation model, or force the continuous solution to both sides of the feasible domain [23].

The first strategy involves reformulation of purity constraints in terms of the reflux split

$$\sum_j \zeta_j^R x_j \leq x_{\text{spec}}. \tag{5.19}$$

As one will always observe a concentration gradient in a finite distillation column, this formulation favours integer solutions as it competes with a lower capital costs which distributes fractions on lower trays. Hence this strategy is assumed to be most successful for steep concentration gradients at either of the column. It should be considered, that this formulation requires the variable tray location to be on the side at which the specified purity lies.

The second approach relies on the previously introduced differentiable distribution function. Here a sufficient focus on a given tray can be enforced by adjusting the underlying standard deviation. By introducing that function in the first optimization stage, while continuing with the traditional formulation in the subsequent steps, convergence could be achieved.

As for the optimization results. It can clearly be seen that both solution approaches return very similar objective values. However somewhat large deviations can be observed in the operational parameters and structural decisions. The deviations given in the results table are based on the results from the outer approximation. The fact that the optimal solutions deviate up to 57 % in certain parameters further strengthes the argument, that due to the highly non-convex nature of the problem only locally optimal solutions are returned. Furthermore large differences can be seen in the computational time.

	amb. air	CR CAC ν	CR main ν	HPC SV 1	LPC SV 1	LPC SV 2	CAC d	HPC d	LPC d
mode 1	14135.58	28.869	4.2016	2064.272	8887.894	570.707	1.09	3.10	4.18
mode 2	14974.81	89.664	4.4796	16.680	9999.85	1702.693	-	-	-

Table 5.7: dual steady-state optimization results - continuous variables.

While the total CPU time is considerably larger for the outer approximation algorithm, the CPU time is smaller. These results however depend heavily on the way the problem is posed. In the course of the thesis several different optimizations have been solved. Some with similar complexity as the cases discussed here. While the NCP always took comparable time for convergence, very large variations were observed, when the outer approximation algorithm was employed. For some cases solution times were even faster than the initial iteration of the NCP. Changes in this behaviour are most likely due to the quality of the linear approximations used to solve the MILP. Drastic changes could be observed when the feasible domain for certain decision variables was adjusted. Furthermore a considerable number of infeasible iterations was observed in the presented case. While in this case infeasible is not meant as violation of constraints but rather failure to converge the underlying process model after solving the MILP. To that regard several observations were made when working with the developed models. As initialization procedures are only carried out when simulating the process and not during optimizations, the solver has to initialize from an available previous solution or a saved variable set. For most cases, when the alteration in the process parameters are not too large, this posed no greater problem. Even changes in stream locations over several stages could be solved from available saved variable sets. However for some integer decisions convergence could fail by changing a stream location by only one tray.

Dual steady-state operation

For a second test case it was assumed, that the plant would have to operate under two distinct operation modes. One requiring a very high nitrogen purity and the other focusing on very pure oxygen. The steady states correspond to the ones from the previous section. To simultaneously consider two steady states, two instances of the process were were considered, that were allowed to differ in terms of operational decisions, but fixed in terms of structural decisions. The structural decisions are all stream locations and diameters. The decision variables correspond to the ones from the previous sections.

This problem could only be converged using the reformulation strategy. The outer approximation algorithm did not converge for this particular case. However it needs to be pointed out, that a very similar case for somewhat less complex scenarios was converged by outer approximation. This particular case however could not even be solved using the optimal solution from the continuous reformulation as an initial guess. Nevertheless it is assumed, that with careful tweaking of the optimization parameters and solver setting convergence could eventually be achieved. Otherwise the same initial point as in the previous section was used to initialize the optimization. The results are summarized in tab. 5.7 and tab. 5.8.

As only one solution approach produced usable results, no comparison can be made as to the quality of the solution. However aside from from solution quality and time consumption, the robustness of a solution algorithm is very important, when it comes to solving complex scenarios. For the examples

	CAC N	HPC N	LPC N	LPC F1	LPC F2	LPC F3	LPC S1	LPC S2
dual SS FB	46	12	44	7	6	21	5	21

Table 5.8: dual steady-state optimization results - discrete variables.

examined in the scope of this thesis, all problems which could be solved by outer approximation, could also be solved using the reformulation as NCP. In contrast, not all scenarios which where the NCP approach yielded a solution, could be solved by outer approximation.

This suggests, that the reformulation strategy has are certain advantages in terms of robustness. It needs to be emphasised, that all findings here are limited to the narrow class of scenarios examined. Due to the limited range of problems, the findings deduced here have no claim for generality. Previous studies have shown [15] that the MINLP formulation of the separation sequence problem often yields (near) integer variables when solved as an NLP. This is due to the fact, that for each feed stream there is a distinct optimal stage. This stage corresponds to the one stage, where the concentration matches the feed concentration as closely as possible. By feeding a stream to such a stage, energy losses due to entropic mixing effects are minimized, and the need for external energy is kept to a minimum. This beneficial effect is not present for other integer decisions. The use of the DDF function or the reformulated purity constraint, as discussed in the previous section is also exclusive to distillation columns.

5.3 Dynamic models

The results of steady-state optimizations give very valuable information about the desired operation of the process in question. In real-live applications however, processes will always display transient behaviour, which cannot be captured by steady-state models. Any given process is required to operate within ceratin bounds and subject to external disturbances, which might cause the process to deviate from desired operations. To be able to handle such disturbances, or in some cases even be able to operate at all at the specified operating point, control structures are required. By the nature of the question aspects of stability or operability can only be analyzed based on a dynamic representation of the system.

The consideration of dynamics further opens the possibility to extend the optimization beyond monetary measures, or consider transient aspects which play a role in process profitability. This might include the optimization of transition times between multiple steady states, or an improved start-up or shut down behaviour. The product streams from a process during transition times often have to be discharged. By optimizing the transition process, one might be able produce marketable or usable product, even during transitions. In case of the ASU which might also be implemented as a utility to a downstream process, the load following behaviour according to utility requirements could also be analyzed.

The remainder of this section is structured as follows. Initially, the dynamic degrees of freedom for the ASU flowsheet are discussed. Subsequently the dynamic process behaviour is analyzed with regards to the sensitivity to external and internal disturbances. Some conclusions are drawn from the observed dynamic effects, encountered particularly in high purity distillation processes.

5.3.1 Degrees of freedom

In order to gain more insight into the behaviour of the dynamic models presented above an analysis of the degrees of freedom within the model is at hand. For the degrees of freedom the cost correlations will be disregarded, as they for a closed system of equations given the inputs generated form the column model. Furthermore interdependencies can be disregarded, as the cost model consist only of "forward" computations. In practical terms this statement can be confirmed since the models can be evaluated with and without costing equations. Hence only the stage and hydraulic equations will be considered.

For a given column without condenser or reboiler the model is made up of $[n_S(5n_C + 24) + n_F]$ differential algebraic equations in $[n_S(5n_C + 29) + n_F(n_S + n_C + 3) + 1]$ variables. In this isolated case all feed flow rates, their composition and enthalpies would be specified. In this case the feeds include a hypothetical condenser reflux (the upper most feed) as well as reboiler reflux (lowest feed). Along with the feeds and their qualities, the feed splits and reflux split have to be assigned. Lastly the column diameter needs to be known. This yields $[n_F(n_S + n_C + 2) + n_S + 1]$ specifications. To close the system initial conditions for all states have to be given. There are a total of $[4n_S]$ dynamic states in a column section.

The condenser reboiler unit is made up of a total condenser and a reboiler side. For the condenser side holdups are neglected. While the reboiler side is modeled much like a column stage. The complete model consists of $[14+6n_C]$ equations in $[17+6n_C]$ variables. The three specified variables would commonly correspond to the condenser pressure, reboiler volume and reflux ratio on the condenser side. While other specifications are conceivable, they cannot be made entirely arbitrarily. A specification on the reboiler pressure for instance would result in a high index problem ($\approx n_S^{LPC}$) which could not be solved without drastically reformulating the model.

5.3.2 Dynamic process behaviour

With the dynamic models a more rigorous approach to analysing the process behaviour is possible. Several aspects of the transient behaviour are of interest. To gain an insight into the process dynamics and test the capabilities of the implemented models, several simulation studies have been conducted.

Especially when dealing with control aspects of a process, the step responses to disturbances in the process are of great interest. Therefore first a study of process reactions to various internal and external disturbances will be conducted. This is followed by a more detailed investigation of some phenomena occurring during process operations.

Step responses

To identify a possible control structure the dynamic interactions of the process have to be analyzed. The most current method of controlling a process would be model predictive control (MPC), where the set point for all manipulated variables are provided by a central controller, which is based on a rigorous process model. In this case however a simpler and in practice still more common approach is

to implement PID control loops. In that case each measured variable is paired with a manipulated variable, which is altered to keep the measured quantity within operational bounds.

Among the most tested tools to synthesize a control structure are the relative gain array (RGA) and block relative gain (BRG). Those tools provide a measure for the interactions within the process. As it is unlikely, that one manipulated variable will only affect the controlled variable it is assigned to. Intuitively, highly integrated processes display strong interactions between all manipulated and measured variables. To analytically calculate the RGA or BRG, a control (linearized) process model in terms of transfer functions is necessary. Alternatively, plant or simulation experiments can be used, to determine the interdependencies within the process. To do so, the process response in the controlled variables to step changes in manipulated variables is examined.

To derive feasible pairings, first all manipulated (u_i) and measured (y_i) variables are identified, based on the previously discussed degrees of freedom. The measured variables correspond to the constraints enforced on the process.

- y_1 : LPC nitrogen purity $\left(y_{1,N_2}^{LPC}\right)$
- y_2 : oxygen product purity $\left(x_{O_2}^{CRmain}\right)$
- y_3 : CAC argon purity $\left(y_{1,Ar}^{CAC}\right)$
- y_4 : nitrogen product flowrate $(\dot{n}_{N_2})$
- y_5 : oxygen product flowrate $(\dot{n}_{O_2})$
- y_6 : argon product flowrate $(\dot{n}_{Ar})$

The manipulated variables are derived from the degrees of freedom analysis.

- u_1 : main air feed flowrate $(\dot{n}_{air})$
- u_2 : CR main reflux ratio $\left(\nu^{CRmain}\right)$
- u_3 : CR CAC reflux ratio $\left(\nu^{CRCAC}\right)$
- u_4 : HPC side stream flowrate $\left(S_1^V\right)$
- u_5 : LPC side stream flowrate 1 $\left(S_1^V\right)$
- u_6 : LPC side stream flowrate 2 $\left(S_2^V\right)$

To analyze the impact of the different manipulated variables, several simulation studies were undertaken. The steady state attained during steady state optimization was taken as nominal operating conditions. To get a feel for the process behaviour, the responses to a 10% step increase in the manipulated variables was simulated. The results are displayed in fig. 5.5.

Before discussing the results in more detail, some comments have to be made as to how these results were attained, and how they are displayed. While for most cases the step response simulation was straightforward, it did lead to errors for the vapour side draw from the high pressure column. To still produce usable data, a steep ramp was used alternatively. Over a time-interval of 10 seconds, the nominal value was increased by ten percent, and remained steady afterwards. To produce a

meaningful and comparable representation of the simulation results, all values for the measured variables were normalized to their respective values under normal operating conditions. Furthermore there are two time scales employed, indicated on the bar below the graphs. All cases were simulated for the span of an entire day, and the step was applied at the very beginning of the simulation. When analysing the results, it turned out, that dynamic effects were taking place on two different scales. While some measured variables were only approaching steady-state at the end of the day, others reached it within about an hour. The different time scales are due to the nature of the measured variables. Pressure associated values such as flowrates change much more quickly, than temperature or concentrations [39]. It also needs to be pointed out, that the y-scales for the graphs differ between measured variables. To maintain some degree or comparability, the y-scales are constant for each measured variable. In the given process configuration, the changes inflicted by the applied steps are of rather low amplitude. For the considered concentrations, the changes to the order of $10^{-}3$ or 0.1 % were observed. Non the less, given these responses, preliminary candidates for coupling between controlled and measured variables can be deduced.

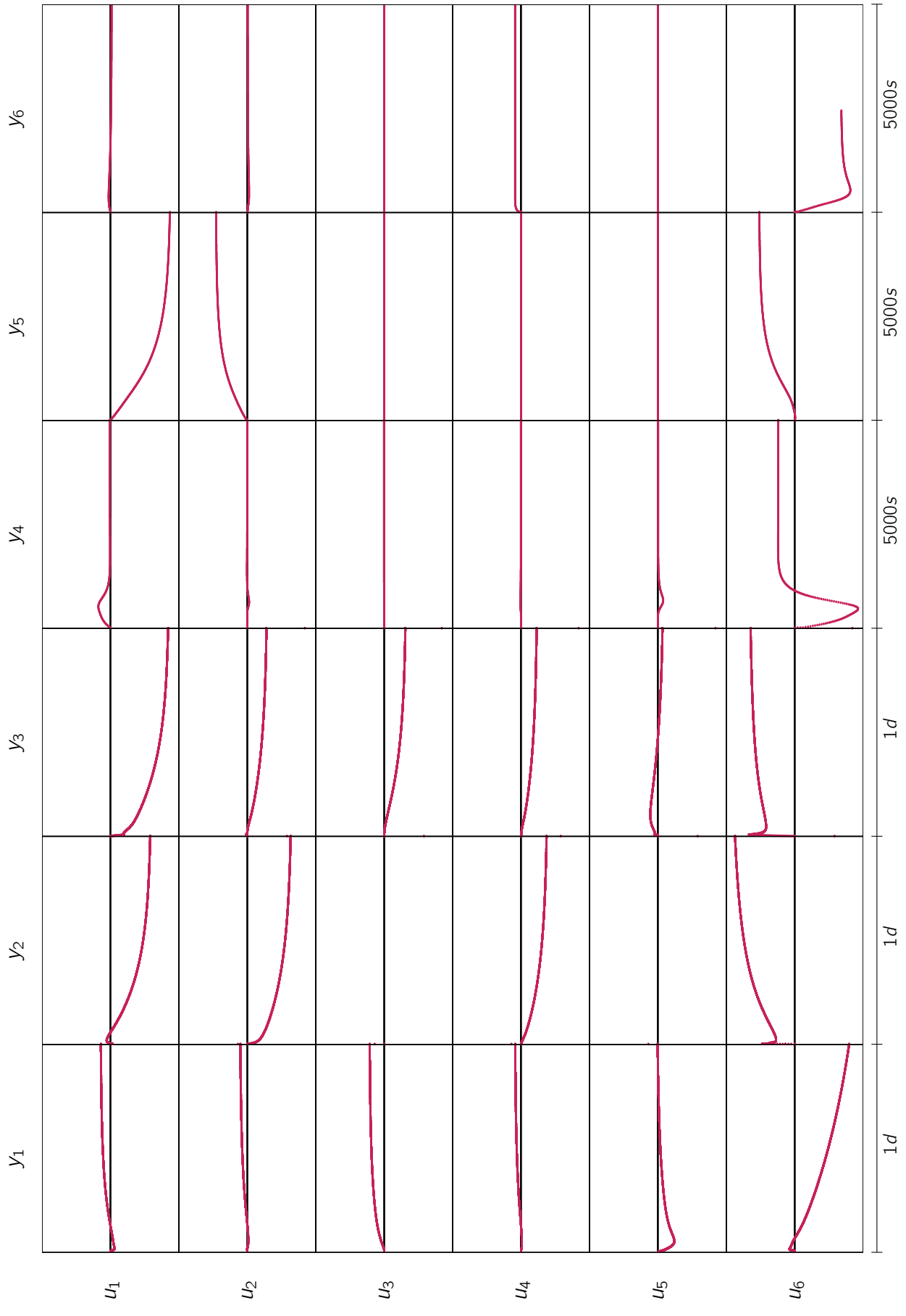

Figure 5.5: step responses.

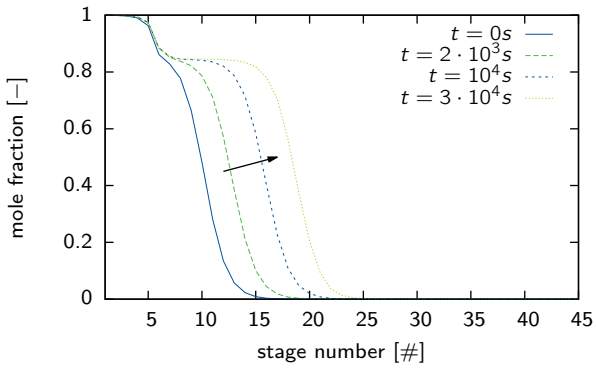

(a) Dynamic profile after feed enthalpy increase.

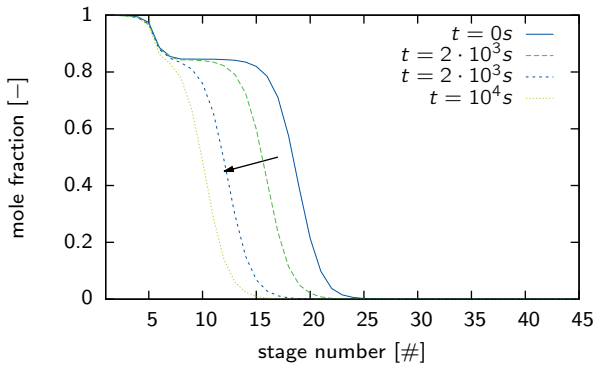

(b) Dynamic profile after feed enthalpy decrease.

Dynamic profiles

The previous section showed only minor reactions to step changes in the manipulated variables. However a closer look at the dynamic column profiles reveals a much different picture. To analyze the internal column behaviour a external disturbance to the feed pressure was applied. As a result, the concentration profiles within the column undergo various changes. Especially with high purity separation sequences, a highly non-linear behaviour with two distinct characteristics is displayed. For one, two time scales can be observed, in which new steady states are reached. Secondly, the transition time between two steady states relies heavily on direction and magnitude of the disturbance [18]. The first effect deals with short- and long-term dynamics, while the second is referred to as asymmetric dynamics.

From this preliminary study, of the dynamic process behaviour, it can be concluded, that an effective control strategy, should not only aim at directly maintaining the the product qualities, but rather to stabilize the internal column profiles. As the effects are often on time scales spanning over a day, there is a chance to detect malicious effects to product specifications in advance and and introduce appropriate counter measures. As can be seen in fig. 5.6a the external disturbance leads to formation of a concentration wavefront within the column. This behaviour is typical for septation processes and be exploited to derive low-order models for control purposes [30]. The fact that this non-linear behaviour is captured by the implemented models, further deepens the trust in the predictive capabilities of the implemented models.

5.4 Model application issues

Aside from the actual model equations care must be taken as to how to implement any set of equations, such that a numerical solver can find feasible solutions. The most prominent issues one is faced with in that context are scaling and singularities within the model. Both aspects will be briefly discussed here.

5.4.1 Scaling

When evaluating a model, or integrating over a given time span, Taylor expansion is used to construct an approximate linear process model. This means, that a system of the form

$$\mathbf{A}x = b, \tag{5.20}$$

is solved to a specified absolute accuracy ε. For a single equation the choice of an appropriate value for ε is rather simple, given that the magnitude of $\mathbf{A}x$ and b is known. Here one needs to consider, that if either magnitude is much grater than ε a large number of iterations will be necessary to solve the system in question. On the other hand, if they are of similar magnitude relative error in the attained solution might become unacceptably high.

To address these issues it is wise to consider the model scaling while implementing the equations. One approach would be to introduce scaling factors on both sides of an equation. While this may certainly improve scaling for the equation itself, the opposite might be true for the respective derivative. Consider the following simple example [29] where to holdups are added to a total holdup

$$f(M_i) = M_1 + M_2 = M_T \tag{5.21}$$

Assuming both holdups are of magnitude $M_1 = M_2 = 10^5 kg$, then the function value is $2 \cdot 10^5$, while for the derivative

$$\frac{\partial f}{\partial M_1} = \frac{\partial f}{\partial M_2} = \frac{\partial f}{\partial M_T} = 1 \tag{5.22}$$

holds. Introducing a scaling factor of 10^{-5} to both sides of the equation would lead to a function value of 2 but have an adverse effect on the derivatives $\frac{\partial f}{\partial M_i} = 10^{-5}$.

A more robust approach would be to scale the units of the given equation which can simultaneously improve scaling for the function and its derivatives. Writing the same equation in tonnes would lead to function value of 200 while maintaining the well scaled derivatives. Alternatively one can introduce further variables and equations with the aim to get more linear equation and rescale some parts of the original equation. A more linear function leads to more constant Jacobian elements and reduces the need for Jacobian updates which can be very expensive in computational terms.

When it comes to the dynamic models, the issue of scaling is extend with another aspect. While for the steady-state models, one could rewrite each equation with different units, as long as each equation is in itself consistent, the same cannot be said, for the dynamic models. Here it is imperative, to maintain the same time scale for every dynamic equation. Due to the very large flow-rates, the steady-state and dynamic balances were written in $\frac{kmol}{hr}$ to achieve a well scaled equation. Considering the various dynamic effects discussed in the previous section, this seems to coarse to capture all relevant phenomena. Maintaining one time unit as one hour would lead to integrator steps of $\frac{1}{3600}$ for one second. Considering furthermore the small changes in the model variables, intuitively this would lead to very badly scaled problems. To somehow accommodate these considerations, it was decided, to introduce a scaling factor solely on the left hand side of the dynamic equations. By those means, the time scale of the process model can easily be adjusted for seconds, minutes, hours or days.

5.4.2 Singularities

Singularities in the models considered here often occur, when a variable is raised to a non-integer power, or the logarithm of a variable is evaluated. Expressions like have no solution within the rational domain, when the respective variable becomes negative. Furthermore when negative exponents are involved a value of zero would lead to a division by zero which is undefined. Even before that the function value might become very large as the variable approaches zero.

In the context of a distillation column, this issue becomes especially relevant, when optimizations or simulations with inactive trays are carried out. Some flowrates in the inactive section of the model will be zero, depending on whether the top or bottom reflux is optimized, those will be either vapour or liquid flowrates. While a solution of zero might cause issues in some cases, a negative solution introduces even more complications. As the equations are solved within numerical accuracy, this might also lead to (slightly) negative solutions, which will cause the numerical solver to fail. Such scenarios have to be anticipated while implementing the model and appropriate measures have to be taken to "protect" such variables from hindering model evaluation.

As gPROMS® supports state transition networks, one way is to introduce conditional statements. However those statements will in almost all cases lead to discontinuities in the model. While in principal such discontinuities can be detected by numerical solvers [35], they are a further source for instabilities. Hence they should in the best case only be introduces, when there is a physical correspondence in the system behaviour.

In this thesis the problem was approached by decoupling the flowrates within the column, and the ones used for evaluation of the hydraulic model. With the help of the split fractions active and inactive trays can be distinguished.

$$V_j^{\text{hyd}} = \left(\sum_{k=1}^{j} \zeta_k^R\right) \cdot V_j + \left(1 - \left(\sum_{k=1}^{j} \zeta_k^R\right)\right) \cdot V_1 \tag{5.23}$$

Here it should be pointed out, that it only needs to be ensured, the the hydraulic model can be evaluated for inactive trays. What results are returned for these trays has no effect for the modelled column operation.

5.4.3 Time scale

The discussion of the dynamic column behaviour revealed, that dynamic effects are occurring on very different time scales. Some are to the order of seconds, others hours and days. Naturally, the finest scale determines the required accuracy. However a very high accuracy leads to an excessive amount of computational time as the model has to be evaluated much more often, as the resolution of the discredited time increases. Furthermore the aspect of model scaling once more has to be considered. As said before, scaling of units is the most effective way, to both scale equations and derivatives. In the case of the ASU process, kmol/hr was selected for the material balances. Hence the dynamic terms are also in terms of hours. This is way too coarse for the purposes of studding the dynamic behaviour. However rewriting the equation in seconds would lead to a (in this particular case) badly scaled equation. In order to retain the well-scaled equation and increase the resolution, a scaling

factor for the dynamic terms was introduced, by which the time scale of the terms was adjusted to seconds. As a side effect, the time scale can be easily adjusted to cater to the specific needs in a simulation. Arguably, there are some issues with accuracy, using the given approach, as in fact the convergence accuracy is reduced to the order of the scaling factor. However it was found to be the most promising solution given the tradeoff between model accuracy and robustness.

6 Conclusion and further research

Within the presented thesis several models have been implemented, which are suitable to be used for process optimization. The most elaborate model concerns distillation columns. Both steady-state and dynamic models have been implemented. The core of these models is formed by the so called MESH equations which denote the energy and material balances along with the governing equations for the vapour liquid equilibrium and a closure condition for the mole fractions.

While these equations are capable of predicting steady-state operations for a given column, there are further aspects of great interest to the process designer. For the dynamic models the column dynamics, in form of hydraulic equations, have to be considered in order to attain a closed model, whereas for the steady state case these can be replaced by respective specifications. Hence these hydraulic equations are implemented as an elective module for these column models. To extend the capabilities of these models other modules have also been added which are elective for both dynamic and steady-state models. Among those are Murphee tray efficiencies, which account for non-equilibrium stages and costing models which yield approximations for an expected size and cost for the simulated columns.

When it comes to simulating unit operations with these models the question of model initialization becomes relevant. Due to the highly non-linear nature of the equation system, the solver needs to be provided with a good initial guess to start convergence to a feasible solution. Complex column configurations with multiple feeds and side draws as well as highly non-ideal mixtures further complicate the matter. To approach this problem the model environment gPROMS® offers initialization procedures which allow to solve a sequence of model variants with increasing complexity. Several approaches suitable for different systems have been implemented.

Process optimization has been the driving force when implementing these models. Especially structural decisions associated with column design such as number of separation stages or feed and side draw locations. The resulting mixed-integer non-linear programs are particularly hard to solve. Convergence is is highly dependent on model robustness and problem formulation. As discussed in sec. **??** the solution of these programs can be approached in several ways. To allow for the the greatest flexibility the model superstructures can be adjusted to have variable top or bottom reflux locations. Furthermore a so called differentiable distribution function can be incorporated to facilitate convergence to a solution.

From the perspective of an industrial end-user of these models, a drag and drop solution which can easily be deployed and yields reliable results is an ideal solution. An effort was made within this thesis to ascertain whether if and how such a drag and drop solution might work.

HX integration model have been developed

Bibliography

[1] Charles O. Akinlabi, Dimitrios I. Gerogiorgis, Michael C. Georgiadis, and Efstratios N. Pistikopoulos. Modelling, Design and Optimisation of a Hybrid PSA-Membrane Gas Separation Process. In V. Plesu and P. S. Agachi, editors, *17th European Symposium on Computer Aided Process Engineering*, volume 24 of *Computer-Aided Chemical Engineering*, pages 363–370, Amsterdam, 2007. Elsevier Science B.V.

[2] Andreas Pfennig. *Thermodynamik der Gemische*. Springer-Verlag, 2003.

[3] Randall F. Barron. *Cryogenic systems*. Oxford University Press and Clarendon Press, New York and Oxford [Oxfordshire], 2 edition, 1985.

[4] Mariana Barttfeld and Pío A. Aguirre. Optimal Synthesis of Multicomponent Zeotropic Distillation Processes. 1. Preprocessing Phase and Rigorous Optimization for a Single Unit. *Industrial & Engineering Chemistry Research*, 41(21):5298–5307, 2002.

[5] J. F. Boston. Inside-Out Algorithms for Multicomponent Separation Process Calculations: AkinlabiAkinlabi. In *Computer Applications to Chemical Engineering*, pages 135–151.

[6] J. F. Boston and S. L. Sullivan. A new class of solution methods for multicomponent, multistage separation processes. *The Canadian Journal of Chemical Engineering*, 52(1):52–63, 1974.

[7] W. F. Castle. Air separation and liquefaction: recent developments and prospects for the beginning of the new millennium. *International Journal of Refrigeration*, 25(1):158–172, 2002.

[8] J. J. J. Chen. Letter to the Editor: Comments on improvement on a replacement for the logarithmic mean. *Chemical Engineering Science*, 42:2488–2489, 1987.

[9] Wan-Kyu Choi, Tae-In Kwon, Yeong-Koo Yeo, Hwaung Lee, Hyung Keun Song, and Byung-Ki Na. Optimal operation of the pressure swing adsorption (PSA) process for CO2 recovery. *Korean Journal of Chemical Engineering*, 20(4):617–623, 2003.

[10] John M. Coulson and Raymond K. Sinnott. *Chemical engineering*. Pergamon Pr., Oxford and and Frankfurt, 3 edition, 1999.

[11] Guido Dünnebier and Constantinos C. Pantelides. Optimal Design of Thermally Coupled Distillation Columns. *Industrial & Engineering Chemistry Research*, 38(1):162–176, 1999.

[12] M. A. Duran and Ignacio E. Grossmann. Simultaneous optimization and heat integration of chemical processes. *AIChE Journal*, 32(1):123–138, 1986.

[13] John Emsley. *Nature's building blocks: An A-Z guide to the elements*. Oxford University Press, Oxford and and New York, 2003, c2001.

[14] Roger Fletcher and William Morton. Initialising distillation column models. *Computers & Chemical Engineering*, 23(11-12):1811–1824, 2000.

[15] Ignacio E. Grossmann, Pío A. Aguirre, and Mariana Barttfeld. Optimal synthesis of complex distillation columns using rigorous models. *Computers & Chemical Engineering*, 29(6):1203–1215, 2005.

[16] J. J. Gualito, F. J. Cerino, J. C. Cardenas, and J. A. Rocha. Design Method for Distillation Columns Filled with Metallic, Ceramic, or Plastic Structured Packings. *Industrial & Engineering Chemistry Research*, 36(5):1747–1757, 1997.

[17] Ernest J. Henley, J. D. Seader, and D. Keith Roper. *Separation process principles*. John Wiley & Sons, Chichester, 3 edition, op. 2011.

[18] Yng-Long Hwang. Nonlinear wave theory for dynamics of binary distillation columns. *AIChE Journal*, 37(5):705–723, 1991.

[19] Ravindra S. Kamath, Lorenz T. Biegler, and Ignacio E. Grossmann. Modeling multistream heat exchangers with and without phase changes for simultaneous optimization and heat integration. *AIChE Journal*, 58(1):190–204, 2012.

[20] Karl Kammermeyer. Technical Gas Permeation Processes. *Chemie Ingenieur Technik*, 48(8):672–675, 1976.

[21] Henry Z. Kister. *Distillation design*. McGraw-Hill, New York, 1992.

[22] Harry Kooijman, Taylor Ross, and Jasper van Baten. The ChemSep/COCO Casebook: Air Separation Unit.

[23] Korbinian Kraemer, Sven Kossack, and Wolfgang Marquardt. Efficient Optimization-Based Design of Distillation Processes for Homogeneous Azeotropic Mixtures. *Industrial & Engineering Chemistry Research*, 48(14):6749–6764, 2009.

[24] Korbinian Kraemer and Wolfgang Marquardt. Continuous Reformulation of MINLP Problems. In Moritz Diehl, Francois Glineur, Elias Jarlebring, and Wim Michiels, editors, *Recent Advances in Optimization and its Applications in Engineering*, pages 83–92. Springer Berlin Heidelberg, Berlin and Heidelberg, 2010.

[25] Y-D Lang and L. T. Biegler. Distributed stream method for tray optimization. *AIChE Journal*, 48(3):582–595, 2002.

[26] M. J. Lockett. *Distillation Tray Fundamentals*. Cambridge Univ Pr, Cambridge and New York, 2009.

[27] A.I Lygeros and K.G Magoulas. Column Flooding and Entrainment. *Hydroc. Proc.*, 65(12):43–44, 1986.

[28] P. Mahapatra and B. W. Bequette. Process design and control studies of an elevated-pressure air separations unit for IGCC power plants: American Control Conference (ACC), 2010: American Control Conference (ACC), 2010 DOI -. *American Control Conference (ACC), 2010*, pages 2003–2008, 2010.

[29] Mark Pinto. Scaling in gPOROMS - training presentation, 2008.

[30] Wolfgang Marquardt. *Nichtlineare Wellenausbreitung: Ein Weg zu reduzierten dynamischen Modellen von Stofftrennprozessen*. VDI Verlag, Düsseldorf [Germany], 1988.

[31] Wolfgang Marquardt. *Prozessentwicklung in der Verfahrenstechnik*. Lecture Notes, Aachener Verfahrenstechnik - Prozesstechnik, RWTH Aachen University, Aachen, 2008.

[32] Thomas Melin and Robert Rautenbach. *Membranverfahren: Grundlagen der modul- und anlagenauslegung*. Springer-Verlag Berlin Heidelberg, Berlin and and Heidelberg, 3 edition, 2007.

[33] Leonard M. Naphtali and Donald P. Sandholm. Multicomponent separation calculations by linearization. *AIChE Journal*, 17(1):148–153, 1971.

[34] Peter R. Nelson. *Oxygen from air by pressure swing adsorption*. PhD thesis, Cape Peninsula University of technology, Cape Town and South Africa, 1993.

[35] Constantinos C. Pantelides. *The Mathematical Modelling of the Dynamic Behaviour of Process Systems*. Lecture Notes, Centre for Process Systems Engineering, Imperial College London, London, 2003.

[36] Max Stone Peters, Klaus D. Timmerhaus, and Ronald E. West. *Plant design and economics for chemical engineers*. McGraw-Hill, New York, 5 edition, 2003.

[37] R. Prasad, F. Notaro, and D.R Thompson. Evolution of membranes in commercial air separation. *Journal of Membrane Science*, 94(1):225–248, 1994.

[38] J. Antonio Rocha, Jose L. Bravo, and James R. Fair. Distillation columns containing structured packings: a comprehensive model for their performance. 1. Hydraulic models. *Industrial & Engineering Chemistry Research*, 32(4):641–651, 1993.

[39] B. Roffel, B.H.L Betlem, and J.A.F de Ruijter. First principles dynamic modeling and multivariable control of a cryogenic distillation process. *Computers & Chemical Engineering*, 24(1):111–123, 2000.

[40] W. D. Seider, J. D. Seader, D. R. Lewin, and S. Widagdo. *Product and Process Design Principles: Synthesis, Analysis, and Evaluation*. J. Wiley, New York, 3 edition, 2010.

[41] Avinash R. Sirdeshpande, Marianthi G. Ierapetritou, Mark J. Andrecovich, and Joseph P. Naumovitz. Process synthesis optimization and flexibility evaluation of air separation cycles. *AIChE Journal*, 51(4):1190–1200, 2005.

[42] A.R Smith and J. Klosek. A review of air separation technologies and their integration with energy conversion processes. *Fuel Processing Technology*, 70(2):115–134, 2001.

[43] Oliver Stein, Jan Oldenburg, and Wolfgang Marquardt. Continuous reformulations of discrete–continuous optimization problems. *Computers & Chemical Engineering*, 28(10):1951–1966, 2004.

[44] Phillip C. Wankat and Kyle P. Kostroski. Hybrid Membrane-Cryogenic Distillation Air Separation Process for Oxygen Production. *Separation Science and Technology*, 46(10):1539–1545, 2011.

[45] T.F Yee and Ignacio E. Grossmann. Simultaneous optimization models for heat integration—II. Heat exchanger network synthesis. *Computers & Chemical Engineering*, 14(10):1165–1184, 1990.

A Simultaneous heat integration

Traditionally heat integration has been carried out in a sequential manner, where it is for the purposes of process optimization assumed, that all heating and cooling is done by external utilities. After an (locally) optimal process configuration is identified, all hot and cold streams within the process are identified, and their temperature intervals fixed. In subsequent steps first the minimum utility requirements, and maximum number of heat exchangers are identified, and a specific heat exchange network (HEN) is designed. While this approach has been successfully applied to a multitude of processes and led to substantial savings, it is questionable if such a sequential approach will yield an optimal or near optimal solution.

Therefore some efforts have been made to develop efficient strategies for simultaneous process optimization and heat integration. Two general approaches can be distinguished. The first one based on the pinch concept. These methods are able to identify the minimum heat requirement as well as stream temperatures during process optimization. The first model along these lines was published by Duran and Grossmann [12] in 1986. They introduced a limited number of quite well behaved constraints into the optimization model to ensure no minimum driving force violations. Recently this model has been extended to handle phase changes and by fixing the utilities to zero been applied to the design of a multi-stream heat exchanger [19]. The major drawback with these methods is that one cannot target area of a given heat exchanger as the approach temperatures are not computed by the model. Therefore the sometimes substantial trade-off between the cost for heat exchange area and utility cost cannot be regarded.

A second approach employs superstructures of a HEN to find optimal matchings of process streams. No pinch point calculations are required, as the actual heat exchange is more or less modeled explicitly. This leads to the benefit, that approach temperatures as well as exchanged heat duties between each stream coupling are known within the model, and the cost of the designed unit can be considered in an economic objective function.

A.1 HEN superstructure

The approach and respective superstructure adapted in this thesis were first published by Yee and Grossmann [45]. Fig. A.1 shows the stage wise superstructure for a HEN consisting of two hot and two cold streams.

In this stage wise structure each hot stream can exchange heat with each cold stream within each stage. The following assumptions were made when the model was developed

- Constant heat capacities

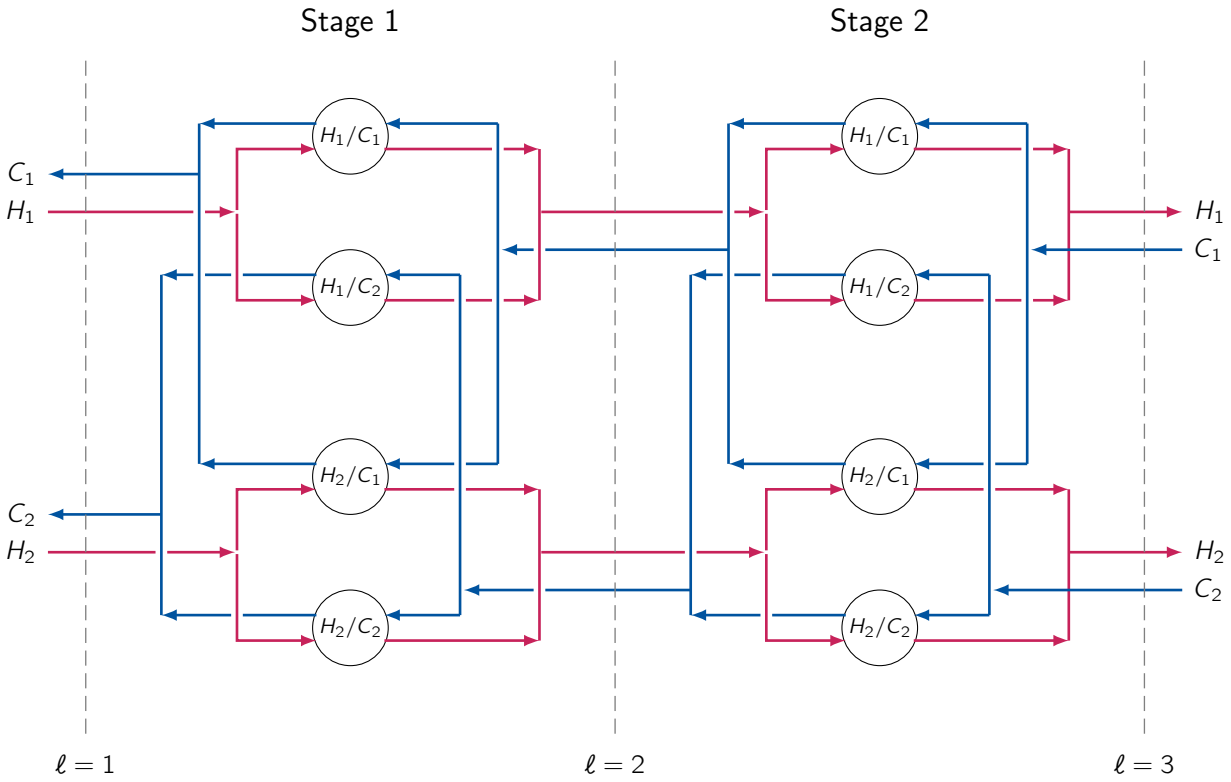

Figure A.1: Superstructure for multi-stream heat exchanger. [45]

- Constant heat transfer coefficients
- Countercurrent heat exchangers
- Isothermal mixing at each stage.

The assumption of constant heat capacities is a common one in the design of HEN's. When no phase boundaries are passed and the temperature range of the involved is not too wide, it is a reasonably good approximation of the real conditions. While constant heat transfer coefficients a re assumed the model leaves the flexibility to define different coefficients for each pairing of hot and cold streams. Countercurrent heat exchangers are common in industrial practice. This assumption however does not really pose a limitation, as the model can easily be altered to account for concurrent units.

The last assumption of isothermal mixing is a more major one. It has been introduced as it allows for significant simplifications and leads to a model, where all constraints are linear and all non-linearities are restricted to the objective function. While that is certainly not true for the entire process model, it should at least allow for some reductions in the model complexity. The assumption states, that regardless of which streams a given stream exchanges heat with, it will leave at the same temperature. Due to that all energy balances around each unit in the superstructure can be eliminated as well as the subsequent mixing of the streams.

Model equations First of all a heat balance at each stage is necessary

$$F_i(T_{i,\ell} - T_{i,\ell+1}) = \sum_j q_{ijk} \tag{A.1}$$

$$f_j(T_{i,\ell} - T_{i,\ell+1}) = \sum_i q_{ijk} \tag{A.2}$$

The heat exchange area A_{hx} can be computed from the exchanged energy, the heat transfer coefficients α_{ij} and the logarithmic mean temperature difference $LMTD$.

$$A_{hx} = \sum_i \sum_j \sum_k \frac{q_{ijk}}{\alpha_{ij} * LMDT_{ijk} + \delta} \tag{A.3}$$

While the small number δ is included to avoid problems in the program, when $LMDT$ becomes zero In order to avoid further numerical difficulties when the approach temperatures ΔT_{ij} at each side of an exchange unit approach zero, it was proposed to use an approximation introduced by Chen [8]

$$LMDT_{ijk} \approx \left[\Delta T_{ijk} \cdot \Delta T_{ijk+1} \frac{\Delta T_{ijk} + \Delta T_{ijk+1}}{2}\right]^{\frac{1}{3}}. \tag{A.4}$$

While the approach temperatures are defined as

$$\Delta T_{ijk} = \max\{0, T_{ik} - T_{jk}\} \tag{A.5}$$

As the max function is non-smooth and thus non differentiable at the points $T_{ik} = T_{jk}$, gPROMS® internally uses a smooth approximation. The exact for of which is unknown to the author.

A.2 Pinch concept based

B Simultaneous control design

C Peng Robinson

C.1 Peng-Robinson derived properties

The Peng-Robinson equation of state cab be rewritten as a cubic polynomial in terms of the compressibility factor $Z = \frac{pv}{RT}$

$$0 = Z^3 + \alpha Z^2 + \beta Z + \gamma \tag{C.1}$$
$$\alpha = B - 1 \tag{C.2}$$
$$\beta = A - 2B - 3B^3 \tag{C.3}$$
$$\gamma = B^3 + B^3 - AB \tag{C.4}$$
$$A = \frac{ap}{(RT)^2} \tag{C.5}$$
$$B = \frac{bp}{RT} \tag{C.6}$$

The *Joule-Thompson* factor cab be expressed as

$$\mu_{JT} = \frac{1}{c_p}\left[T\left(\frac{\partial v}{\partial T}\right)_p - v\right] \tag{C.7}$$

and in terms of the compressibility factor

$$\left(\frac{\partial v}{\partial T}\right)_p = \frac{R}{p}\left[T\left(\frac{\partial Z}{\partial T}\right)_p + Z\right] \tag{C.8}$$
$$\left(\frac{\partial Z}{\partial T}\right)_p = \frac{\left(\frac{\partial A}{\partial T}\right)_p (B - Z) + \left(\frac{\partial B}{\partial T}\right)_p (6BZ + 2Z - 3B^2 - 2B + A - Z^2)}{3Z^2 + 2(B-1)Z + (A - 2B - 3B^2)} \tag{C.9}$$
$$\left(\frac{\partial A}{\partial T}\right)_p = \frac{p}{(RT)^2}\left(a' - \frac{2a}{T}\right) \tag{C.10}$$
$$\left(\frac{\partial B}{\partial T}\right)_p = \frac{-bp}{RT^2} \tag{C.11}$$
$$a' = \frac{da}{dT} = \frac{1}{2}\sum_{i=1}^{C}\sum_{j=1}^{C} w_i w_j (1 - k_{ij})\left(\sqrt{\frac{a_j}{a_i}}a'_i + \sqrt{\frac{a_i}{a_j}}a'_j\right) \tag{C.12}$$
$$a'_i = \frac{da_i}{dT} = \frac{-m_i a_i}{\left[1 + m_i(1 - \sqrt{\frac{T}{T_{ci}}})\right]\sqrt{T T_{ci}}} \tag{C.13}$$

$$\ln \varphi = \frac{1}{RT} \int_0^p \left(V - \frac{RT}{p} \right) dp, \tag{C.14}$$

$$\ln \varphi = (Z-1) - \ln Z - \int_\infty^V \frac{Z-1}{V} dV \tag{C.15}$$

$$\ln \varphi_i = \frac{b_i}{b}(Z-1) - \ln \left[Z \cdot \left(1 - \frac{b}{V} \right) \right] + \frac{1}{bRT} \left[\frac{\sqrt{2} a b_i}{4b} - \sqrt{\frac{a a_i}{2}} \right] \ln \left(1 + \frac{b}{V} \right) \left(\frac{1 + \frac{b}{V}\left(1+\sqrt{2}\right)}{1 + \frac{b}{V}\left(1-\sqrt{2}\right)} \right) \tag{C.16}$$